REPORT DOCUMENTATION PAGE

Form Approved OMB NO. 0704-0188

1. REPORT DATE (DD-MM-YYYY)	2. REPORT TYPE	3. DATES COVERED (From - To)
09-07-2012	Final Report	1-Sep-2011 - 31-May-2012

4. TITLE AND SUBTITLE
Report of STIR Proposal on the Dynamics and Control of Mechanical Energy Propagation in Granular Systems

5a. CONTRACT NUMBER
W911NF-11-1-0437

5b. GRANT NUMBER

5c. PROGRAM ELEMENT NUMBER
611102

6. AUTHORS
Surajit Sen

5d. PROJECT NUMBER

5e. TASK NUMBER

5f. WORK UNIT NUMBER

7. PERFORMING ORGANIZATION NAMES AND ADDRESSES
State University of New York (SUNY) at Buffalo
Sponsored Projects Services
The Research Foundation of SUNY on behalf of Univ at Buf
Buffalo, NY 14260 -

8. PERFORMING ORGANIZATION REPORT NUMBER

9. SPONSORING/MONITORING AGENCY NAME(S) AND ADDRESS(ES)
U.S. Army Research Office
P.O. Box 12211
Research Triangle Park, NC 27709-2211

10. SPONSOR/MONITOR'S ACRONYM(S)
ARO

11. SPONSOR/MONITOR'S REPORT NUMBER(S)
60670-EG-II.5

12. DISTRIBUTION AVAILIBILITY STATEMENT
Approved for Public Release; Distribution Unlimited

13. SUPPLEMENTARY NOTES
The views, opinions and/or findings contained in this report are those of the author(s) and should not contrued as an official Department of the Army position, policy or decision, unless so designated by other documentation.

14. ABSTRACT
The STIR project focused on a set of highly challenging problems to set the stage for future work at a deeper level. These problems are (i) to design a circuit system that simulates the transformation of an incident impulse into a solitary wave, (ii) to study how the width of a solitary wave depends on the geometry of the grain-grain contacts, (iii) how to make solitary waves in noisy environments, (iv) to find what kind of physical situations precipitate large energy fluctuations in nonlinear systems and (v) how to model the presence of fluids in the inter-stitial space

15. SUBJECT TERMS
Solitary waves, Circuits, Quasi-equilibrium, Granular Bed

16. SECURITY CLASSIFICATION OF:			17. LIMITATION OF ABSTRACT	15. NUMBER OF PAGES	19a. NAME OF RESPONSIBLE PERSON
a. REPORT	b. ABSTRACT	c. THIS PAGE			Surajit Sen
UU	UU	UU	UU		19b. TELEPHONE NUMBER: 716-645-2007

Report Title

Report of STIR Proposal on the Dynamics and Control of Mechanical Energy Propagation in Granular Systems

ABSTRACT

The STIR project focused on a set of highly challenging problems to set the stage for future work at a deeper level. These problems are (i) to design a circuit system that simulates the transformation of an incident impulse into a solitary wave, (ii) to study how the width of a solitary wave depends on the geometry of the grain-grain contacts, (iii) how to make solitary waves in noisy environments, (iv) to find what kind of physical situations precipitate large energy fluctuations in nonlinear systems and (v) how to model the presence of fluids in the inter-stitial space between grains in a 3D granular bed. All of these tasks have either been accomplished or have seen substantial progress during the period of this exploratory study. The report details the findings.

Enter List of papers submitted or published that acknowledge ARO support from the start of the project to the date of this printing. List the papers, including journal references, in the following categories:

(a) Papers published in peer-reviewed journals (N/A for none)

Received Paper

TOTAL:

Number of Papers published in peer-reviewed journals:

(b) Papers published in non-peer-reviewed journals (N/A for none)

Received Paper

TOTAL:

Number of Papers published in non peer-reviewed journals:

(c) Presentations

Number of Presentations: 0.00

Non Peer-Reviewed Conference Proceeding publications (other than abstracts):

Received Paper

TOTAL:

Number of Non Peer-Reviewed Conference Proceeding publications (other than abstracts):

Peer-Reviewed Conference Proceeding publications (other than abstracts):

Received Paper

TOTAL:

Number of Peer-Reviewed Conference Proceeding publications (other than abstracts):

(d) Manuscripts

Received		Paper
2012/07/05 15	2	. Sustained strong fluctuations in a nonlinear chain at acoustic vacuum: Beyond equilibrium, ( )
2012/07/05 15	3	. Long Lived Solitary Wave in a 1D Granular Chain, ( )
2012/07/05 15	4	. Nonlinear grain-grain forces and the width of the solitary wave in granular chains: a numerical study, ( )

TOTAL: 3

Number of Manuscripts:

Books

Received	Paper

TOTAL:

Patents Submitted

Patents Awarded

Awards

BS Honors, Dept of Physics Outstanding undergraduate award to WIlliam D Pineros who did an Honors thesis under the PI.

Graduate Students

NAME	PERCENT_SUPPORTED	Discipline
Yoichi Takato	0.35	
Matthew Westley	0.35	
William J Falls	0.20	
Nicholas DeMeglio	0.10	
FTE Equivalent:	**1.00**	
Total Number:	**4**	

Names of Post Doctorates

NAME	PERCENT_SUPPORTED
Huang Decai	0.00
FTE Equivalent:	**0.00**
Total Number:	**1**

Names of Faculty Supported

NAME	PERCENT_SUPPORTED	National Academy Member
Surajit Sen	0.10	
FTE Equivalent:	**0.10**	
Total Number:	**1**	

Names of Under Graduate students supported

NAME	PERCENT_SUPPORTED	Discipline
William D Pineros	0.00	Physics
FTE Equivalent:	**0.00**	
Total Number:	**1**	

Student Metrics

This section only applies to graduating undergraduates supported by this agreement in this reporting period

The number of undergraduates funded by this agreement who graduated during this period:	1.00
The number of undergraduates funded by this agreement who graduated during this period with a degree in science, mathematics, engineering, or technology fields:	1.00
The number of undergraduates funded by your agreement who graduated during this period and will continue to pursue a graduate or Ph.D. degree in science, mathematics, engineering, or technology fields:	1.00
Number of graduating undergraduates who achieved a 3.5 GPA to 4.0 (4.0 max scale):	1.00
Number of graduating undergraduates funded by a DoD funded Center of Excellence grant for Education, Research and Engineering:	0.00
The number of undergraduates funded by your agreement who graduated during this period and intend to work for the Department of Defense	1.00
The number of undergraduates funded by your agreement who graduated during this period and will receive scholarships or fellowships for further studies in science, mathematics, engineering or technology fields:	0.00

Names of Personnel receiving masters degrees

NAME
Total Number:

Names of personnel receiving PHDs

NAME
Total Number:

Names of other research staff

NAME	PERCENT_SUPPORTED
FTE Equivalent:	
Total Number:	

Sub Contractors (DD882)

Inventions (DD882)

Scientific Progress

Technology Transfer

Task (i): Collaborative development of a circuit system that is capable of accepting an input pulse and converting it to the traveling solitary wave pulse seen in a granular alignment (***Solitary Wave Chip Problem***).

The write up below describes our accomplishments in constructing a Simulink version of the granular chain.

Simulink Modeling of Granular Chains (Robert W. Newcomb, Department of Electical and Computer Engineering, University of Maryland, College Park, Maryland 20742 USA (newcomb@eng.umd.edu)
Surajit Sen, Physics Department, State Univesity of New York, Buffalo, New York, 14260 (sen@buffalo.edu))

Abstract—After a review of the coupled Newton's equations for a granular alignment, the equations are put into block diagrams of Simulink. Simulink simulations are given for 22 grain systems with cubic and for Hertz potential energy. The expected granular solitary waves are seen in the simulations.

I. Introduction

The types of grains under consideration comprise a one-dimensional chain of symmetric elastic grains such that an input pulse travels through compression along the chain. By experiment [1], [2], through simulations [3], and by series approximations [4], [5], the pulses are known to be able to form into solitary waves and since action potentials are solitary waves, these are similar to the signals used by biological neurons [6, p. 42] and of considerable interest for mimicking neural information processing. Therefore, these grains can be seen as an alternate means of forming the pulses used in silicon based pulse coded neural networks [7]. Alternatively, their equations can be put into a form which allows for an equivalent transistor structure having the key properties of the elastic spherical grains. Consequently, with an ultimate goal of mimicking the grains behavior in transistor circuits, in this paper we present a Simulink model of these grains in a form that allows for future conversion into VLSI circuits.

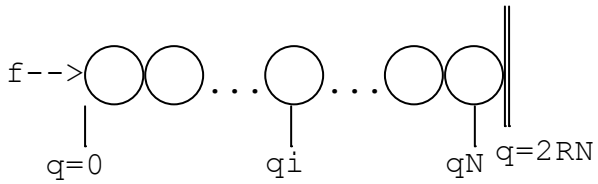

Figure1. Chain of grains of radii R placed between rigid walls.

II. DESCRIBING EQUATIONS

Figure 1 gives a one-dimensional representation of the granular spheres which we here assume all have the same radius R. We consider N grains with q_i being the coordinate of the center of the i^{th} grain. For i=1 an external impulse-like force is assumed applied while for the final grain, at x_N, a rigid wall is assumed. We use the Hamiltonian, H(p,q) representation where p = momentum N-vector and q = position N-vector and H is the sum of the kinetic and the potential, V(.,.), energies. Thus

$$H(p,q) = \sum_{l=l}^{N} \left(\frac{1}{2m} p_i^2 + V(q_{i-1}, q_i)\right) \qquad (1a),$$

$$p_i = m\frac{\partial q_i}{\partial t}, \qquad (1b),$$

$$V(q_{i-1}, q_i) = k[(q_{i-1} + R) - (q_i - R)]_+^{r+1} \qquad (1c)$$

Here q_i is the position of the center of the i^{th} grain measured from an origin q_1-R = 0. The potential energy depends on the overlap, 2R-($q_i - q_{i-1}$), of two adjacent grains if positive (and is zero if there is no overlap). If the rest position is q_{io} and the displaced position is $x_i = q_i - q_{io}$ then the overlap is x_{i-1}-x_i, which gives the potential energy V if positive with V being zero if there is no overlap. So, following [3] the modified symbol $[x]_+ = (x+|x|)/2=(1+\text{sign}(x))x/2$ is used in (1) to designate x if x > 0 and zero if x < 0. The power r+1 is due to Hertz [8] and known to be 5/2 for elastic spheres though we simulate with other r as well [9]; especially r = 2 is convenient for analytic investigations. We set up the equations with r as a parameter which then becomes easy to change in Simulink. The mass of a grain is m and k comprises various constants including Young's modulus.

Simulionk realizations are most easily obtained through the state variable equations which in this case are the Hamilton differential equations.

$$\frac{\partial q_i}{\partial t} = \frac{\partial H}{\partial p_i} = \frac{1}{m} p_i = \frac{1}{m}\frac{dq_i}{dt} \qquad (2a)$$

$$\frac{\partial p_i}{\partial t} = -\frac{\partial H}{\partial q_i} = m\frac{\partial^2 q_i}{\partial t^2} \qquad (2b)$$

By normalizations, the choice of x_i, and introducing possible loss (by the parameter k_{loss}) we recast these into the following state-variable form which are the actual ones we put into Simulink in the following paragraphs.

$$\frac{dx_i}{dt} = z_i \qquad (3a),$$

$$\frac{dz_i}{dt} = \frac{d(\frac{dx_i}{dt})}{dt}, \qquad (3b)$$

$$= (\frac{k}{2^r m})\{((1+\text{sign}(x_{i-1}-x_i))(x_{i-1}-x_i))^r$$

$$-((1+\text{sign}(x_i-x_{i+1}))(x_i-x_{i+1}))^r\} - k_{loss} z_i.$$

Equations (3) are for i = 2, …, N while at i = 1 an additive input term, f(t), is to be added and the x_0 term omitted while at i = N a fixed boundary is imposed by fixing $x_{N+1} = (2N+1)R$. However, since the differences of position hold, the x_i can be interpreted as the incremental displacement of the center of the i^{th} sphere. For solitary waves of velocity c we have $x_i(t) = u(x_i\text{-}ct)$. Following normalizations of Chatterjee [3], this gives the second order differential equation for the solitary wave

$$\ddot{u} = [u(t+1)-u(t)]_+^r - [u(t)-u(t-1)]_+^r. \qquad (4)$$

From these Chatterjee shows MatLab simulations indicating the existence of solitary waves while Sen & Manciu [4] give a series solution approximation. In detail, [5], with α = xi-ct and n a parameter.

$$u(\alpha, n)) = \frac{A}{2}(1 - \tanh(F(\alpha(n))) \qquad (5a),$$

$$F(\alpha, n)) = \frac{1}{2}\sum_{q=0}^{\infty} C_{2q+1}(n)\alpha^{2q+1} \qquad (5b).$$

The C_{2q+1} have been evaluated for q = 0,…,5 and the results shown to be solitary type waves (see Fig. 3.1 of [5]). In short these grains are known to support solitary waves.

Consequently we know that we can obtain solitary waves from the state variable equations (3) so it is to them we turn for possible transistor realization. Toward that we obtain next a suitable block diagram realization.

III. Simulink Block Diagrams

Although we simulate for much larger N, for convenience of illustration Fig. 2 shows a Simulink block diagram for N=5 stages of grains with the sub-blocks for i=2,3,4 being given in detail by Fig. 3 where we have allowed for different grain radii but choose R=0 for equal size grains and x as displacement around equilibrium (the choice of x_i=qi is possible with nonzero R in this setup). The input, i=1, and output, i=N=5, stages are given in Figs. 4 & 5. Figure 3 realizes equations (3) while the input and output stages, are simple modifications reflecting their different loading. In Fig. 2 an input pulse is applied on the left to the input stage.

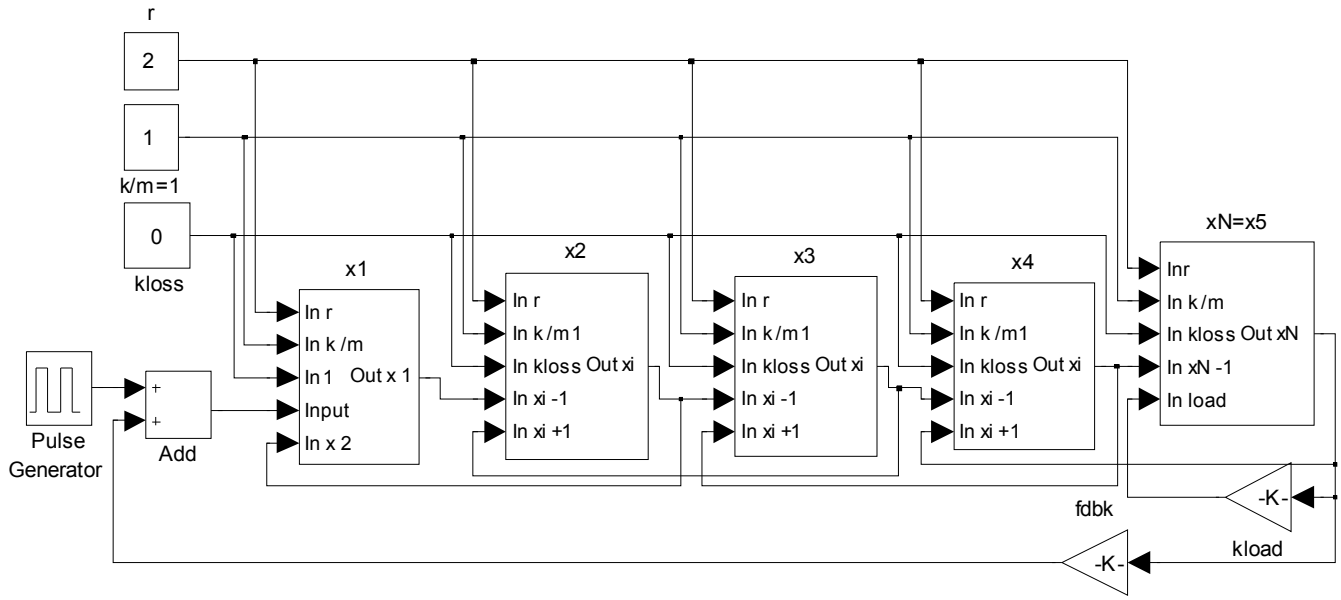

Figure 2. Simulink 5 grains Simulink block connection

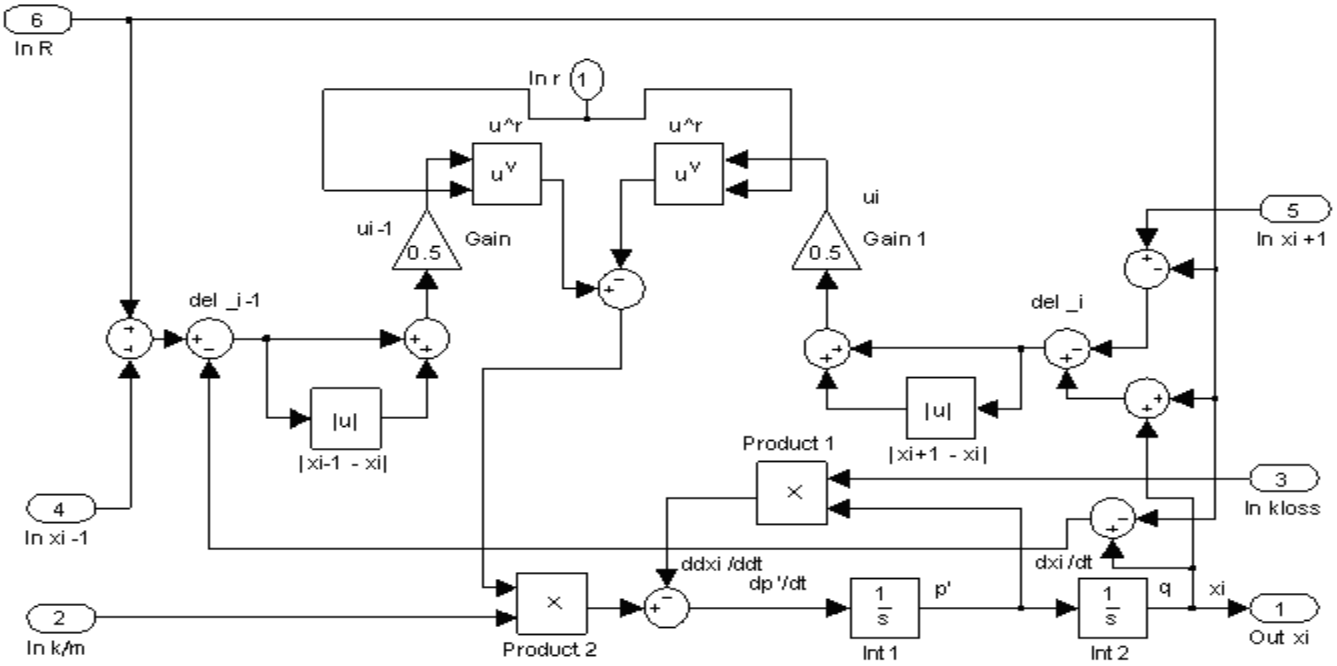

Figure 3. Simulink i^{th} internal grain stage

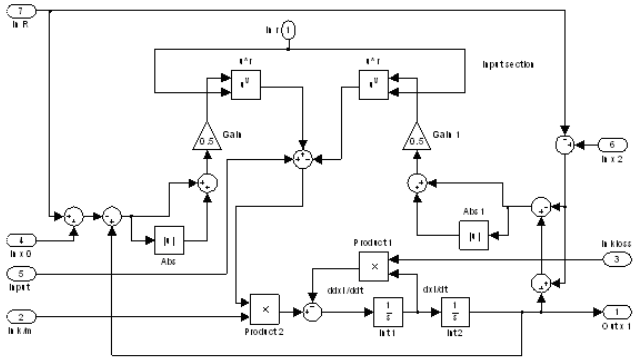

Figure 4. Detailed Simulink input grain, i=1, stage

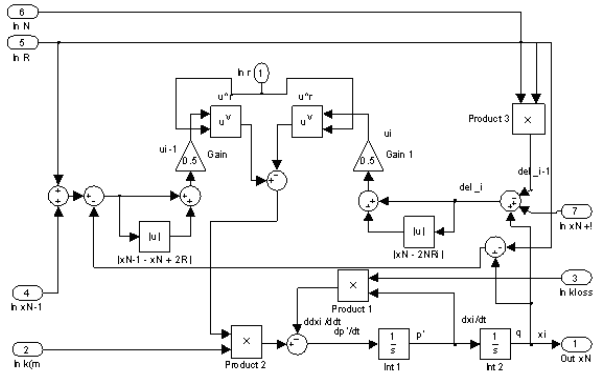

Figure 5. Detailed Simulink output grain stage, i=N

IV. Simulation Results

Figure 6(at the end of the paper) gives a plot of dx/dt at the fourth and the 21st stages for r=2 and m/k normalized to 1, showing solitary waves as well as their reflection from the N=22 end wall. For Fig. 6 a square input pulse of amplitude 10^{-6} and pulse width t=5x10. This results in a traveling wave of amplitude $3.5x10^{-9}$ with a delay of t=2,500 at the 4th grain, for r=2. A reflected wave can be seen at t=32,000 with the solitary pulse arriving at the 21st grain at t=15,000, all in normalized time.

V. Discussion

For obtaining Simulink models we have put the grains differential equations into state variable form, (3) above. From these we are able to set up block diagrams which use only integrators, multipliers, square roots, and summers. These are conveniently put into Simulink through which we have again shown that solitary signals can be generated. In the case of grains satisfying the Hertz potentials these blocks necessitate square roots in obtaining the 3/2 power. However, from the simulations we obtain

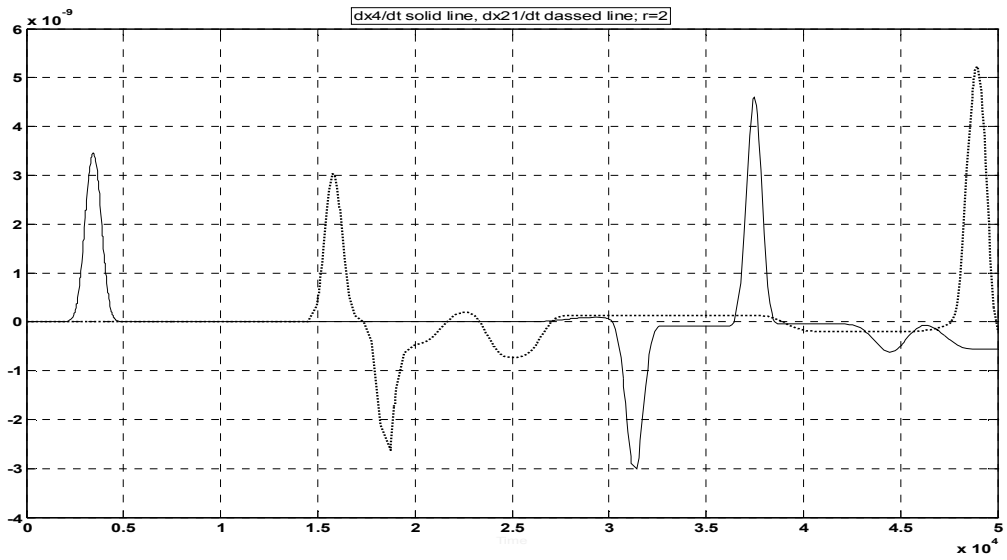

similar results for powers of r=2 as well as 3/2, though with a different time scaling as for example the 4th stage peak occurs at t=200 for r = 3/2. We have normalized m/k=1 and considered x_i as the change in displacement, but we can consider it alternatively as the absolute center position, q_i, of the ith grain; we have chosen the former for the given block diagrams (which also use R=1 for the right wall). In the Simulink system we have the capability of Figure 6. Simulation result:for r=2; solid line dx/dt at 4thgrain ; dashed line dx/dt at 21st grain both for N=22 grain using any real r as well as the added possibility of including loss, though it is not present in the basic grains equations. The above can be generalized to allow for different radii and for different materials of different individual grains within the system, and this is allowed for by separate ports in the individual grain cell blocks.

Some useful additional references are included [10-20]. For example, there are other effects which can be included, one of which uses the "coefficient of restitution" [11], while generalization to higher dimensions is possible, such as for sand at the beach. Also the above equations are normalized though denormalization is easily carried out. ([20]] gives material constants for various materials).

Acknowledgment

The authors wish to acknowledge Professor Krishna Shenai of the University of Toledo for bringing them together on this problem. SS acknowledges support of an US Army Research Office - STIR grant.

VI. REFERENCES

Vitali F. Nesterenko, "Propagation of Nonlinear Compression Pulses in Granular Media," Journal of Applied Mechanics and Technical Physics, Vol. 24, No. 5, pp. 733 – 743, 1983.

C. Coste, E. Falcon and S. Fauve, "Solitary waves in a chain of beads under Hertz contact," Physical Review E Vol. 57, pp. 6104-6117, 1997.

Anindya Chatterjee, "Asymptotic solution for solitary waves in a chain of elastic spheres," Physical Review E, Vol. 59, No. 5, pp. 5912 – 5919, 1999.

Surajit Sen, Marian Manciu, and James D. Wright, "Soliton-like pulses in perturbed and driven Hertzian chains and their possible applications in detecting buried impurities," Phys Rev E Vol. 57, 2386-2397, 1998.

Surajit Sen and Marian Manciu, "Solitary wave dynamics in generalized Hertz chains: An improved solution of the equation of motion," Physical Review E, Vol. 64, pp. 056605-1 – 056605-4, 2001.

William F. Ganong, "Review of Medical Physiology," Lange Medical Publications, Los Altos, CA, 1985.

Mona E. Zaghloul, Jack L. Meador, and Robert W. Newcomb, "Silicon Implementation of Pulse Coded Neural Networks," Kluwer Academic Publishers, Boston, 1994.

Heinrich Hertz, "Ueber die Beruehrung fester elastischer Koerper," Journal fuer die reine and angewandte Mathematik, Vol. 92, pp. 156 – 171, 1881. See page 168 for the 5/2 power law.

Diankang Sun, Chiara Daraio, and Surajit Sen, "The nonlinear repulsive force between two solids of revolution," Physical Review, Vol. 83, pp. 066605-1 - 06605-5., 2011.

Surajit Sen, Jongbae Hong, Jonghun Bang, Edgar Avalos, and Robert Doney, "Solitary waves in the granular chain," Physics Reports Vol. 462, No. 2, pp. 21 – 66, 2008.

Goro Kuwabara and Kimitoshi Kono, "Restitution Coefficient in a Collision between Two Spheres," Japanese Journal of Applied Physics, Vol. 26, No. 8, August, pp. 1230 – 1233, 1987

Stephane Job, Francisco Melo, Adam Sokolow and Surajit Sen, "How Hertzian solitary waves interact with boundaries in a 1D granular medium," Physical Review Letters, Vol. 94, pp. 178002-1-178002-4, 2005.

Surajit Sen and Marian Manciu, "Discrete Herzian chains and solitons," Physica A: Statistical Mechanics and Applications, Vol. 268, Nos. 3-4, June 15, pp. 644 – 649, 1999.

Marian Manciu, Surajit Sen and Alan J. Hurd, "Impulse propagation in dissipative and disordered chains with power-law repulsive potentials," Physica D: Nonlinear Phenomena, Vol. 157, No. 3, September 15, pp. 226 – 240, 2001.

E. Falcon, B. Castaing, and M. Creyssels, "Nonlinear electrical conductivity in a 1D granular medium," The European Physical Journal B, Vol. 38, Nol. 3, pp. 475 – 483, 2004.

F. Hermann and P. Schmaeizle, "Simple explanation of a well-known collision experiment," American Journal of Physics, Vol. 49, No. 8, August, pp. 761 – 764, 1981

F. Herrmann and M. Seitz, "How does the ball-chain work?," American Journal of Physics, Vol. 50, No. 11, November, pp. 977 – 981, 1982

Robert Paul Simion, "Nonlinear Granular Breathing," Doctoral dissertation, Department of Physics, State University of New York at Buffalo, May 2010.

Vitali F. Nesterenko, "Dynamics of heterogeneous materials," Springer, New York, 2001.

Jinkyu Yang, Claudio Silvestro, Devvrath Khatri, Luigi De Nardo and Chiara Daraio, “Interaction of highly nonlinear solitary waves with linear elastic media,” Physical Reiew E, Vol. 83, pp. 045505-1 – 046606-12, 2010

Task (ii): Developing a heterogeneous granular alignment system that can compress or dilate propagating solitary waves (***Solitary Wave Width Control Problem***).

Width of the Solitary wave in granular alignments (Diankang Sun, Yoichi Takato, Nicholas DeMeglio and Surajit Sen, SUNY Buffalo)

Solitary waves (we denote solitary wave as SW throughout) that are about 5 grain diameters wide naturally form in a chain of unloaded elastic spheres that repel with overlap as $V(\delta_{i,i+1}) = a\delta_{i,i+1}{}^{n}, \quad \delta \geq 0,$ where for spheres n = 5/2.[Nesterenko 1983, Lazaridi and Nesterenko 1985, Sen and Manciu 2001, Sokolow, et al, 2007, Sen, et al, 2008] For $n \to 2$ and $n \to \infty$, a one-sided harmonic 1D chain of cylindrical or disk shaped beads and a chain of particles with hard-sphere-like repulsion are approached respectively. It is known that for $n > 2$ an impulse propagates in these systems as solitary waves [Nesterenko 1983, LN 1985, Sen et al, 2008] The width W of these solitary waves are known to depend only upon n but a detailed understanding of $W(n)$ has not been available. Here we use numerical and analytical methods to study how the SW width depends on n. In the numerical study, a geometric tool is employed to calculate the total time averaged kinetic energy of the SW by using the virial Theorem. The idea is to construct an isosceles triangle area such that its area equals that of the SW. Hence the base of the triangle gives the width of the SW. We then analytically explore the width of the SW. Here we present the results of a detailed computational and theoretical study to propose, $W(n) \propto (n-2)^{-\alpha}$, where $\alpha \approx 1/3$.

Introduction

Now consider an alignment of elastic grains that are held between fixed, rigid walls that would perfectly reflect energy. The grain-grain potential is described for convenience as

$$V(\delta_{i,i+1}) = a_n\delta_{i,i+1}{}^{n}, \quad \delta \geq 0, \qquad (1)$$

where $a_n = \left(\frac{Y}{1-\sigma^2}\right)\left(\frac{R^{3-n}}{2^{n-3}n(n-1)}\right)_2 F_1(n-2,2-n;n-1;1)$ and is a constant given by the material and the geometric properties of the grain, Y and σ are the Young's modulus and Poisson's ratio, and δ denotes the overlap of two adjacent grains.

We start by considering the equation of motion of a bead in the chain,

$$m\frac{d^2u_i(t)}{dt^2} = na_n\left\{ \left[\Delta_i + u_{i-1}(t) - u_i(t)\right]^{n-1} - \left[\Delta_i + u_i(t) - u_{i+1}(t)\right]^{n-1}\right\} \qquad (2)$$

where Δ_i is the pre-compression effected on the grain in the chain. Sound propagation is not admissible when there is no preloading, i.e., when $\Delta_i = 0$. This is because when $n > 2$, the right hand side (RHS) of the equation cannot be Taylor expanded. So there is no quadratic term that is admissible on the RHS, which implies that there are no harmonic oscillations [Nesterenko, 1983, Nesterenko, 1985, Chatterjee, Sen, 1999, 2001]. Hence no sound propagation is possible. u_i denotes the displacement of the grain i from its equilibrium position. High-precision numerical studies show that the discrete chain systems admit robust solitary waves propagating through the chain with a unique wave width. These studies also reveal that the wave width depends only on n (Manciu et al, 1999a). A perturbation that is sufficiently weak such that only elastic compressions of grains are involved results in the eventual formation of a solitary wave (SW) as discussed in Sokolow et al 2007.

Earlier work of Nesterenko has claimed using continuum theory that

$$W = \frac{2\pi R}{n-2}\sqrt{\frac{n(n-1)}{6}} \quad . \qquad (3)$$

So, when $n \to 2$, $W \to \infty$ (no SW). This is an expected result because $n = 2$ is the acoustic case. When $n \to \infty$, $W \approx 2R$, which is the extreme hard sphere limit when W shrinks to its minimum.

Earlier numerical study using exhaustive dynamical simulations (see Fig. 4 of Manciu, Sen and Hurd, 1999) suggest that Nesterenko's formula for W may need some improvement.

The correction is important because the width formula is sometimes used to find the effective "*n*" in the experiments. Hence this formula is potentially useful in designing granular meta-materials (Daraio, private communication).

Numerical study

We carried out our simulations by setting the masses of the grains $m = 2.314 \times 10^{-2}$ kg, *n* = set of values from 2.001 to 7.0, potential prefactor *a* = 52.442 N/mm$^{1.5}$ for all *n*'s. Although a_n depends on *n* as we have seen in Sun, Daraio and Sen, Phys. Rev. E 83, 066605 (2011), the reason we can use one constant is because each run is independent of the other such that the underlying physics does not change. Further, since we expect W to depend on "n", the choice of the value of a_n is a matter of convenience. We also set □ = 0 so there are no harmonic terms. We used the velocity Verlet algorithm for integrating the coupled equations of motion. The integration time step was taken to be □t = 10^{-5} □s. In the simulation a delta function perturbation with $E_{tot} = \frac{1}{2} m v_0^{\,2} = 0.115715 J$ was initiated at grain 1 at t=0. We set dissipation to zero. Energy was constant through the 10^6 steps of our simulations to one part in 10^6.

We observed the formation of a single solitary wave — a results first reported by Sokolow et al. (Sokolow 2007). Snapshots of a propagating SW at two different times are shown below in Fig. 1, where KE of the grains vs. grain positions are shown for a propagating SW at two different times. The center grain is well defined when the wave consists of an odd number of grains whereas the center is roughly at the edges of the two center grains for a SW sitting on an even number of grains. Nevertheless, the total energy does not disperse even though the SW oscillates between the two widths. To choose either an odd or an even numbered wave width to be the solitary wave width is then a choice of definition. See Fig. 1. we have chosen the odd numbered solitary wave width to represent the width here.

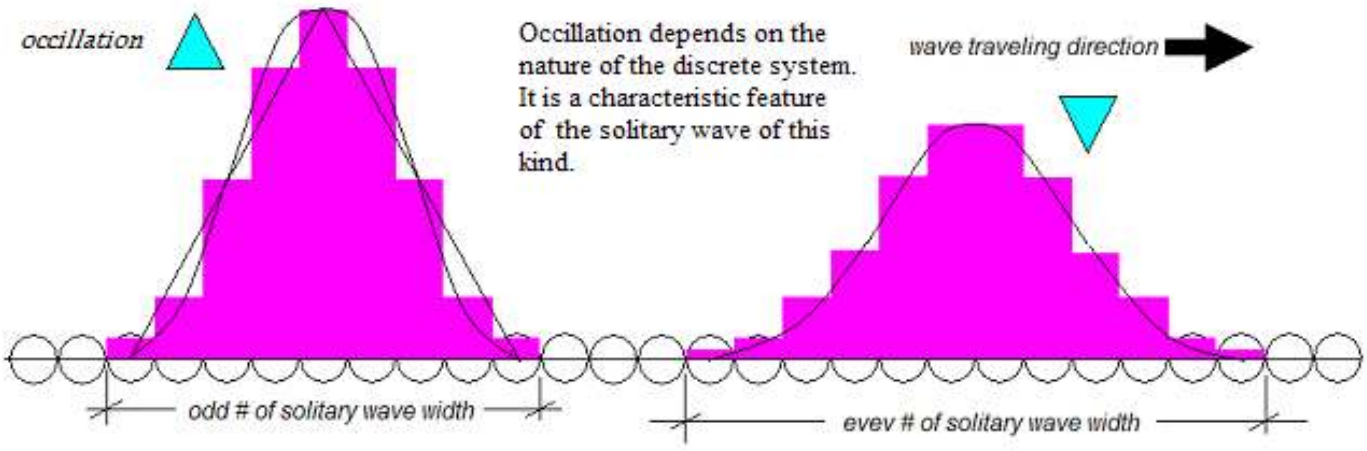

Fig. 1. Solitary wave is traveling with a characteristic fluctuation in width.

Fig. 1 shows that the width of the SW, i.e., the number of grains that a propagating SW sits on, varies slightly and so does the SW amplitude. This makes sense because in a particulate system there would be time periods in which the grains will get more compressed and when they would be less compressed against each other. Increased compression would mean high potential energy whereas smaller compression would mean high kinetic energy. This is the reason why the SW height and spatial extent varies in the KE vs. grain number snapshots in Fig. 1. Thus we focus on the average width of the SW, and our $W \equiv \frac{1}{N}\sum_{i=1}^{N} W_i(t)$, where N is total number of discrete sampling times. Since the width varies with time, we may also define the width of the SW as $W \equiv \frac{1}{t_2 - t_1}\int_{t_1}^{t_2} W(t)dt$.

Numerical results show that as the exponent n decreases (but still greater than 2) the wave hump tends to flatten out, i.e., the width of the SW increases (see Fig. 2). In our numerical studies we choose to keep the total energy of the system and hence of the SW to be the same in every case we examine. The kinetic and the potential energies of the solitary wave then end up being related by the Virial theorem.

The Virial Theorem is generally valid for classical energy conserved systems. Virial Theorem [Goldstein, 2002] says that

$$< KE >= -\frac{1}{2} < \sum_i \vec{F_i} \cdot \vec{r_i} >= -\frac{1}{2} < \sum_i \frac{\partial V}{\partial x_i} \cdot x_i > \ , \qquad (4)$$

where $\vec{F_i}$ is the force on particle *i* located at $\vec{r_i}$ and < > signifies a time average.

In the granular alignment,

$$V \sim \delta^n \sim (u_i - u_{i+1})^n \ ,$$

and for for generalized Hertz-type potentials

$$\langle KE \rangle = \frac{n}{n+2} E_{tot} \ , \text{ and } \langle PE \rangle = \frac{2}{n+2} E_{tot} \ , \qquad (5)$$

and these two results have been confirmed by all of our simulations (see Fig. 1* below).

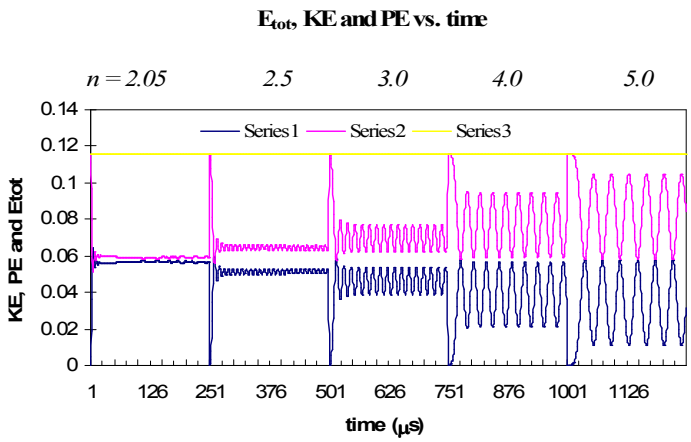

Fig..1* KE and PE vs. time for different *n*'s: 2.05, 2.5, 3.0, 4.0 and 5.0 from left to right.

Now kinetic energy can be determined as a function of *n*, if E_{tot} of the system is known. Hence the descriptions, including the width, of the SW can be fully obtained through the numerical studies of the system. However, as we shall see, the relation of the SW width to its kinetic energy is not trivial to determine

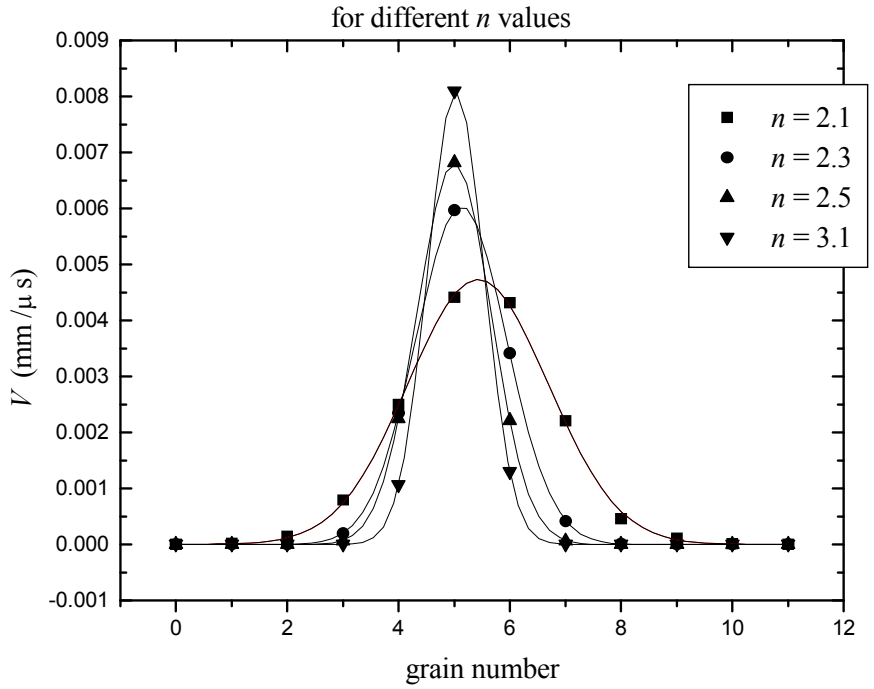

Fig. 2 Some numerical results of the numerical solutions to the equations of motion showing the velocity of the solitary waves for different magnitudes of n. The bigger the n is, the narrower the solitary wave is.

It is difficult to exactly define the width W of a SW. In experiments and in simulations, the width is related to the accuracy with which measurement is possible. In continuum theory the width may diverge. Our calculations show that the grain-grain distance between the grains inside a solitary wave may differ by as many as six decades. It is hence necessary to introduce a reasonable cut-off in some appropriate parameter (displacement or velocity say) to precisely define W.

We in the following present the detailed steps for calculating the width W. The method involves the symmetry property of SW. It says a SW shape is line-symmetric about its center, see Fig. 3. The vertical axis represents the velocity squared of each grain involved in the SW.

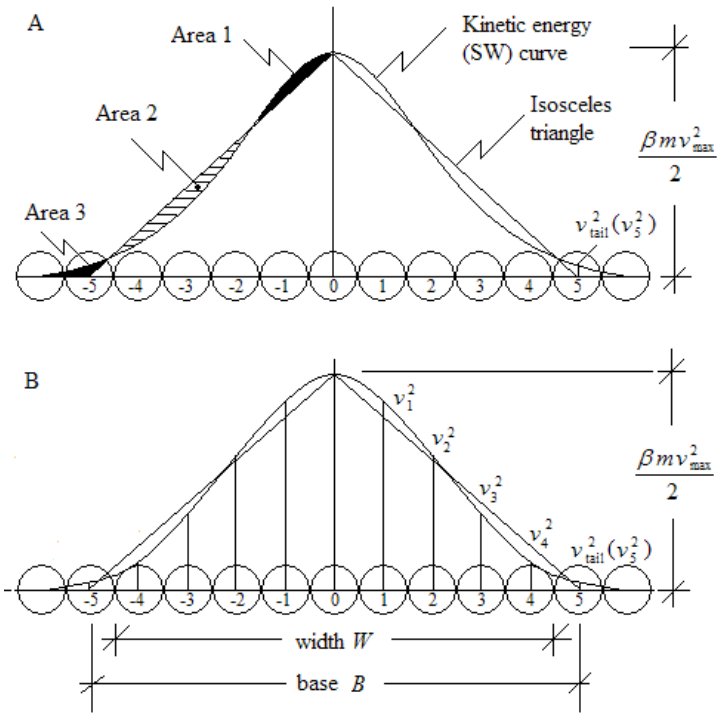

Fig.3. Sketch of the SW being replaced by the isosceles triangle. Panel A illustrates that $Area1 + Area3 = Area2$ where $Area3$ is very small compared with total area of the triangle. One can always construct such an isosceles triangle whose area is equal to that under the solitary wave curve.

Virial Theorem (Eq. (5)) allows us to write

Area of the triangle x m/2 = KE $_{total}$ *= n E* $_{total}$ */ (n+2),* (6)

where *m* is the mass of each grain.

Expressed now in 2-D coordinates *x-y*, the area of the triangle is (see Fig. 3-panel B)

$$A = \frac{1}{2} B(\frac{1}{2} m v_{\max}^2) = \frac{1}{4} B m v_{\max}^2 \ , \qquad (7)$$

which is the total kinetic energy of the solitary wave, i.e.

$$\frac{1}{4} B m v_{\max}^2 = KE = \sum_{i=-\infty}^{\infty} \frac{1}{2} m v_i^{\ 2} \approx \sum_{i=-\frac{W}{2}}^{\frac{W}{2}} \frac{1}{2} m v_i^{\ 2} \ , \qquad (8)$$

where $B = W + 1$. Making use of equation (4) and the definition of $B = W + 1$, we have the width expression,

$$W = \frac{4n}{n+2}\left(\frac{E_{tot}}{mv_{\max}^2}\right) - 1. \qquad (9)$$

Eq. (9) allows us to find the width of a SW for a given index *n*; the known total energy of the system, and the center grain's velocity (which is the maximum velocity) as obtained from the numerical solutions.

Recall that the total energy of the system is $E_{tot} = \frac{1}{2} m v_0^{\,2}$, where v_0 is the initial velocity imparted to the first grain at t = 0, therefore one can also write the width equation in terms of v_0 as follows

$$W = \frac{2n}{n+2}\left(\frac{v_0^{\,2}}{v_{\max}^{\,2}}\right) - 1. \qquad (10)$$

Eq. (10) provides the relation between the SW width and the power law potential exponent *n* given the initial impulse velocity v_0 and the maximum velocity $v_{\max}$ of the center grain of the grains that carry the SW.

Once v_{max} is known from the numerical simulation result, the width of the SW for a given potential component *n* can be obtained. This process can be repeated indefinitely until all studies of widths for different magnitudes of *n* are completed. The width depends upon the magnitude of exponent *n* in the following way: $n \to \infty$, $W \to 1$, i.e., rigid hard potential limit; and $n \to 2$, solitary wave breaks down, i.e., harmonic potential limit.

Our exhaustive numerical studies (see Fig. 4) of such physical systems have shown that the width depends solely upon the potential exponent *n*, and is consistent with a scaling law,

$$W = A_0 (n-2)^{-\alpha} + 1, \qquad (11)$$

in which α_{num} = 0.3301, and the pre-factor A_0=4.5262. A_0 is a constant that only depends on the cutoff threshold energy. We studied *W* for various *n* values. Our simulations confirm that $W \propto (n-2)^{-0.3301}$ or

$W \propto (n-2)^{-1/3}$ where the index 1/3 is approximate. We are unable to further clarify whether the actual index is 1/3 or not.

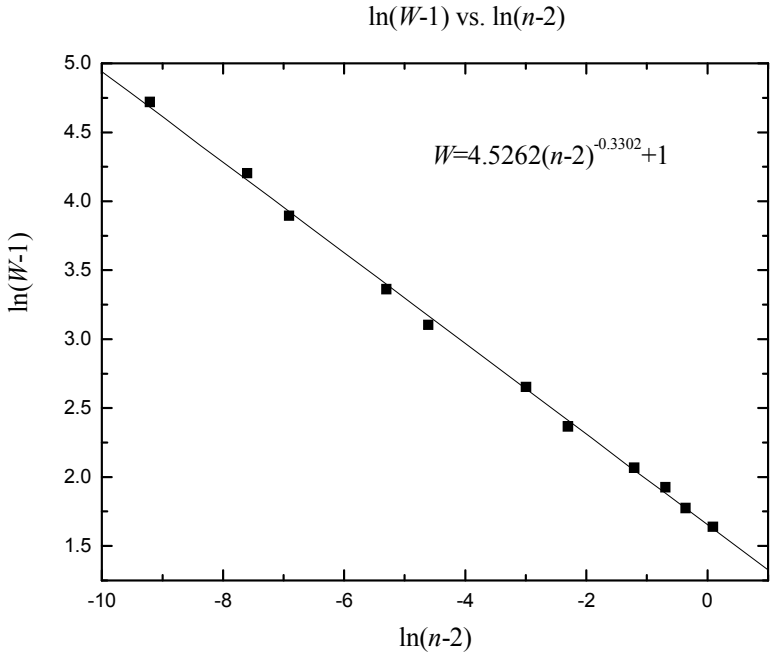

Fig.4. We show a ln-ln plot of *W*-1 vs. *n*-2. The width W depends on *n* as: $W = 4.5262(n-2)^{-1/3} + 1$

Analytical Study

In 2001, Sen and Manciu proposed a series solution for the equation of motion. The solution is as follows:

$$u_i(t) = u(z_i, t) = u(z_i - ct) \equiv u(\alpha) \equiv A\phi_n(\alpha) \qquad (12)$$

where $\alpha \equiv z - ct$, c = velocity of SW. Then we define

$$u(\alpha) = \frac{A}{2}[\phi_n(\alpha) + 1], \quad \phi_n(\alpha) = -\tanh\left(\frac{f_n(\alpha)}{2}\right) \qquad (13)$$

and

$$f_n(z') = \sum_{q=0}^{\infty} c_{2q+1}(n) z'^{2q+1}, \text{ where } z' = z - ct \qquad (14)$$

So knowledge of $c_{2q+1}(n)$ solves $u(z\text{-}ct)$ which reveals the displacement of every grain within the SW and hence solves the equation of motion. $\overset{\circ}{u}(z-ct)$ can hence be found and <KE> and <PE> can in principle be obtained. The following table lists the constants $C_{1\sim5}$ for different n values [Sen 2001]. The constant $C_0 = \dfrac{mc^2}{na_n\left(\dfrac{A}{2}\right)^{n-2}}$, where a is from Eq. (1).

Table 1 Coefficients *C* values for different *n*'s

	n=2.2	2.35	2.5	3.0	4.0	5.0
C0	0.8709	0.6908	0.85852	0.9445	1.3323	2.0517
C1	1.643	2.3171	2.3953	3.0168	3.5646	3.79001
C3	0.08223	0.2364	0.26852	0.5971	1.331	2.177
C5	0.000326	0.003407	0.006134	0.0376	0.0676	0.0665

In the following we report analytical results of SW widths dependence on *n* and how we construct an analytical expression of this SW.

We will now analytically obtain the average potential energy <*PE*> of the SW. The displacement of involved grains from equilibrium positions has the form [Sen 2001],

$$u_i(z_i - t_i) = \frac{1}{1 + e^{f_n(z_i - t_i)}}, \qquad (15)$$

where $f_n(z_i - t_i) = \sum_{q=0}^{\infty} C_{2q+1}(n)(z_i - t_i)^{2q+1}$ is a controlling factor containing all the information of this type of solitary wave, and z_i [= □□□±□□□±□□□□□□□□□±□*W*- 1) / 2] denotes discrete dimensionless coordinate recording the grain number, t_i is a characteristic time, i.e., $t_i = \dfrac{t_{real}}{t_0}$ ($t_0 \equiv$ time for solitary wave to travel one grain diameter) which is not necessary to be discrete. Knowledge of the coefficients $C_0, C_1, C_3, C_5, \cdots$, [6] will completely solve the problem of pulse propagation for any system

supporting this type of SW. One must resort to numerical methods for computing these coefficients. For a certain time t_i, say 0 for convenience we choose $u_i(z_i)$ to be centered at the origin so,

$$u_i(z_i) = \frac{1}{1+e^{f_n(z_i)}}, \tag{16}$$

which leads to the overlap of $\delta_{i,i+1}$ of two adjacent grains,

$$\delta_{i,i+1} = u_i(z_i) - u_{i+1}(z_{i+1}) \tag{17}$$

Hence the potential energy is,

$$\langle PE \rangle = \sum_{i=-\infty}^{\infty} a_n \delta_{i,i+1}{}^n \approx \sum_{i=-\frac{W}{2}}^{\frac{W}{2}} a_n \delta_{i,i+1}{}^n, \tag{18}$$

where $a_n = \left(\frac{Y}{1-\sigma^2}\right)\left(\frac{R^{3-n}}{2^{n-3}n(n-1)}\right)_2 F_1(n-2,2-n;n-1;1)$. For the sake of convenience, we let

$\left(\frac{Y}{1-\sigma^2}\right)R^{3-n} = 1$, hence $a_n = \left(\frac{1}{2^{n-3}n(n-1)}\right)_2 F_1(n-2,2-n;n-1;1)$.

The kinetic energy of the SW likewise can be found as follows,

$u_i(t_i) = \frac{1}{1+e^{-f_n(t_i)}}$, (note that f_n is an odd function) (19)

which gives,

$$v_i(t) = \frac{du_i}{dt} = \frac{\left[\sum_{q=0}^{\infty}(2q+1)C_{2q+1}(n)\ t^{2q}\right]e^{-f_n(t)}}{\left(1+e^{-f_n(t)}\right)^2} \quad . \tag{20}$$

Therefore the kinetic energy is,

$$\langle KE \rangle = \sum_{i=-\infty}^{\infty} \frac{m}{2} v_i{}^2 \approx \sum_{i=-W/2}^{W/2} \frac{m}{2} v_i{}^2, \tag{21}$$

where m is set to be unity.

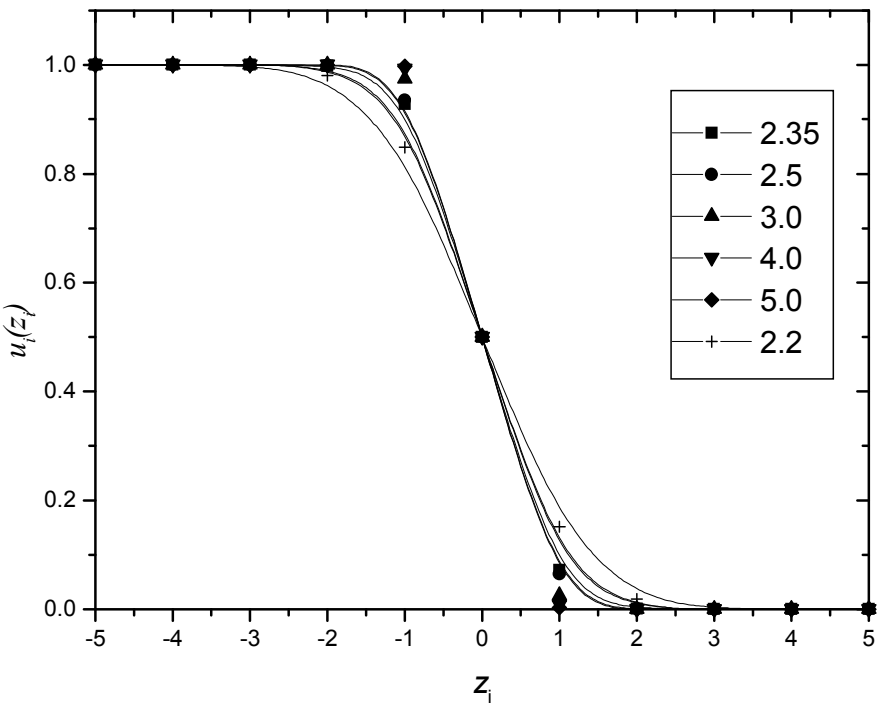
1.0
0.8
0.6
0.4
0.2
0.0
$u_i(z_i)$
-5
-4
-3
-2
-1
0
1
2
3
4
5
z_i
2.35
2.5
3.0
4.0
5.0
2.2

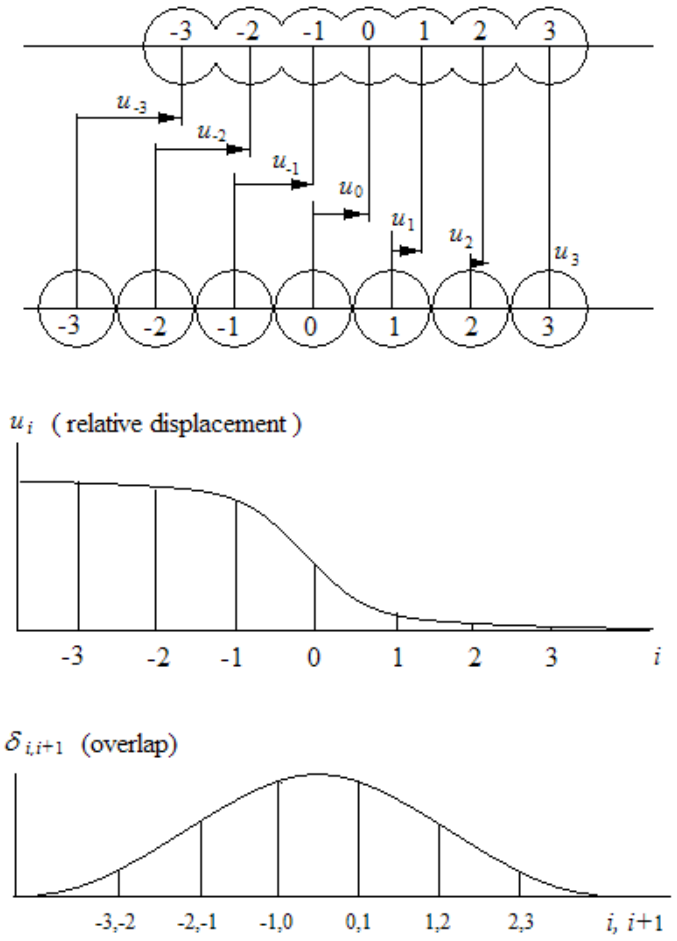

Fig.5 The figure is showing the relative displacement of each bead in a solitary wave, and the compressions (overlaps) of pairs of neighboring beads which constitute a compression solitary wave.

With the knowledge of coefficients $C_1, C_3, C_5, \cdots,$ to desired accuracy, the SWs potential and kinetic energies can thus be calculated for all various n values. Hence the widths have been determined. The accuracy in our studies is to one part in 10^{20}. We calculated 8 data sets of $\delta_{i,i+1}$ at different times to get < $\delta_{i,i+1}$ > shown in Table 2 below.

Table 2. Relative displacements for different *n* values

$<\delta_{i,i+1}>$ (au)	*n* =2.2	*n* =2.35	*n* =2.5	*n* =3.0	*n* =4.0	*n* =5.0	*z*
□□□□□	0	3.2449E-23	7.88E-29	1.011E-90	1.8E-172	2.167E-217	-6
□□□□□	5.18961E-06	7.7427E-13	4.44E-15	2.764E-39	5.62E-74	2.1527E-97	-5
□□□□□	0.000719994	7.0716E-07	1.21E-07	1.26E-15	4.12E-28	3.2861E-38	-4
□□□□□	0.018086981	0.0013119	0.000796	6.061E-06	2.19E-09	1.6602E-12	-3
□□□□□	0.132344218	0.07065122	0.063974	0.0252896	0.006942	0.00239133	-2
□□□□	0.348843614	0.42803616	0.43523	0.4747043	0.493058	0.49760867	-1
□□□	0.348843614	0.42803616	0.43523	0.4747043	0.493058	0.49760867	0
□□□	0.132344262	0.07065122	0.063974	0.0252896	0.006942	0.00239133	1
□□□	0.018086937	0.0013119	0.000796	6.061E-06	2.19E-09	1.6603E-12	2
□□□	0.000719995	7.0716E-07	1.21E-07	1.258E-15	4.12E-28	3.2861E-38	3
□□□	5.18942E-06	7.7434E-13	4.44E-15	2.764E-39	5.62E-74	2.1527E-97	4
□□□	0	3.2449E-23	7.88E-29	1.011E-90	1.8E-172	2.167E-217	5
width	9	7.8	7	5.8	4.6	4.4	

To ensure the width found by the guidance of cutoff ratio of $\delta_{tail} / \delta_{\max} < 10^{-8}$ is correct, *W* must also satisfy the following relations

$$< KE >|_W = \left(\frac{n}{n+2}\right) E_{tot}, \text{ and } \quad < PE >|_W = \left(\frac{2}{n+2}\right) E_{tot} \quad \text{or} \quad \frac{< KE >}{< PE >} = \frac{n}{2} \qquad (22)$$

The following table lists the *KE, PE* and E_{tot} for different *n* values.

Table 3. KE and PE for different *n* values

n	2.2	2.35	2.5	3	4	5
<KE> (arb.u)	0.291317543	0.52372503	0.961398518	1.349544303	2.092941065	2.426093359
expected <KE>/<PE>	1.1	1.175	1.25	1.5	2	2.5
<PE> (arb.u)	0.265464687	0.44678467	0.77095005	0.900839184	1.048962129	0.972747909
calculated <KE>/<PE>	1.097387173	1.17220903	1.247030879	1.498096804	1.995249406	2.494061758
Etot (arb.u)	0.55678223	0.9705097	1.732348568	2.250383487	3.141903195	3.398841267
Prefactor(arb.u)	0.208729714	0.22953622	0.528041	4.204658362	0.474399649	0.513896586

It is clearly seen that the Eqs. (22) are satisfied closely. The plot of expected <KE>/<PE> vs. calculated <KE>/<PE> shows the same agreement (see Fig. 6)

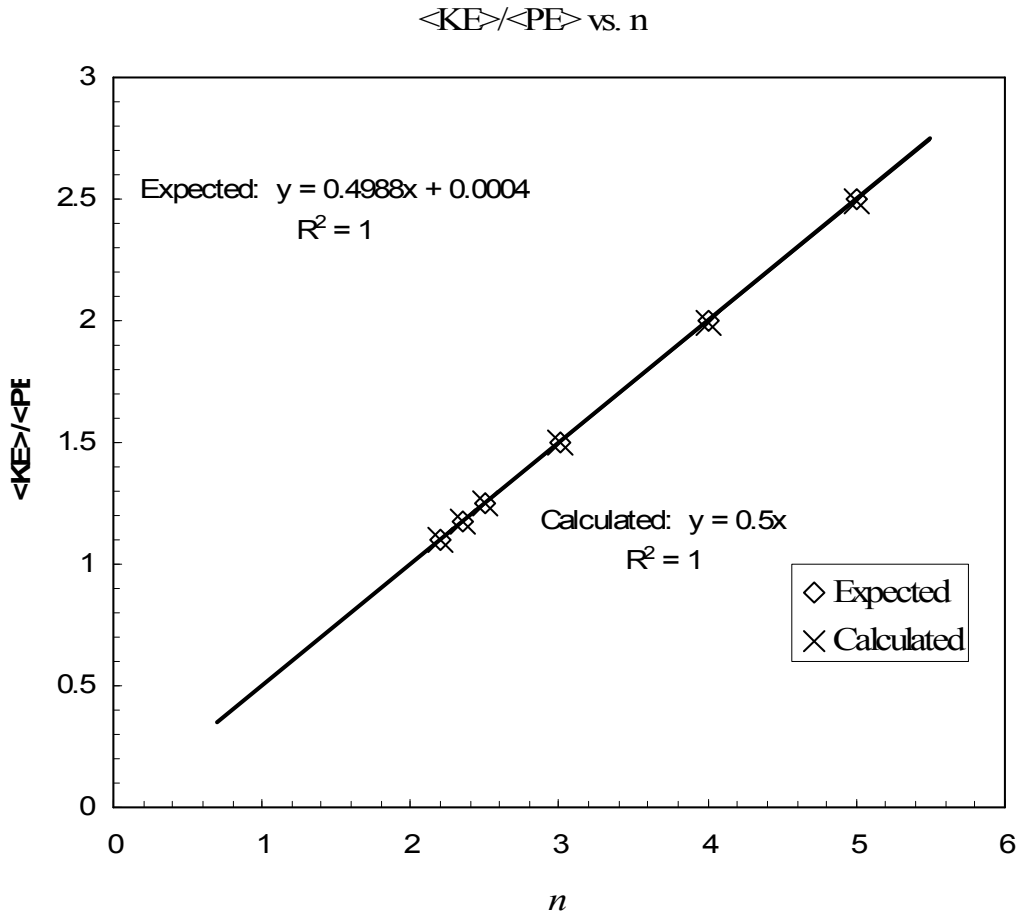

Fig. 6. Both calculated and expected <KE>/<PE> match closely vs. different *n*'s.

It turns out that (see the plot of *W* vs. *n* shown in Fig..7) dependence of *W* on *n* is

$$W = 4.745(n-2)^{-0.3307} + 1, \qquad (22)$$

which agrees with the results obtained by the numerical approach.

The solution is approximate because $C_1, C_3, C_5, \cdots$ used is an infinite series.

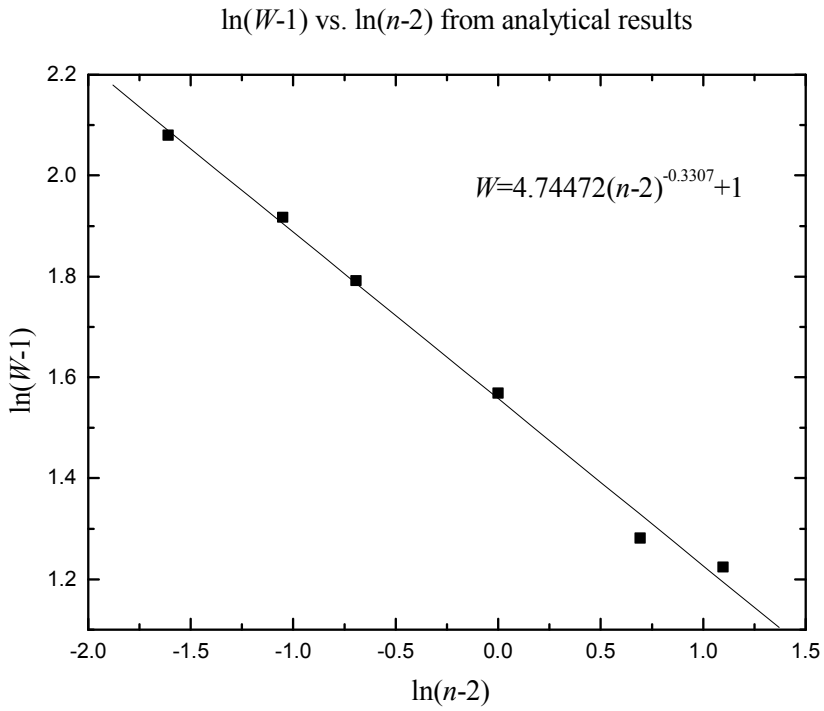

Fig.7. The widths of PE SW being calculated and plotted against n. The ln-ln plot of W-1 vs. n-2 shows the width: $W = 4.745(n-2)^{-0.3307} + 1$, which provides a good agreement with the scaling law.

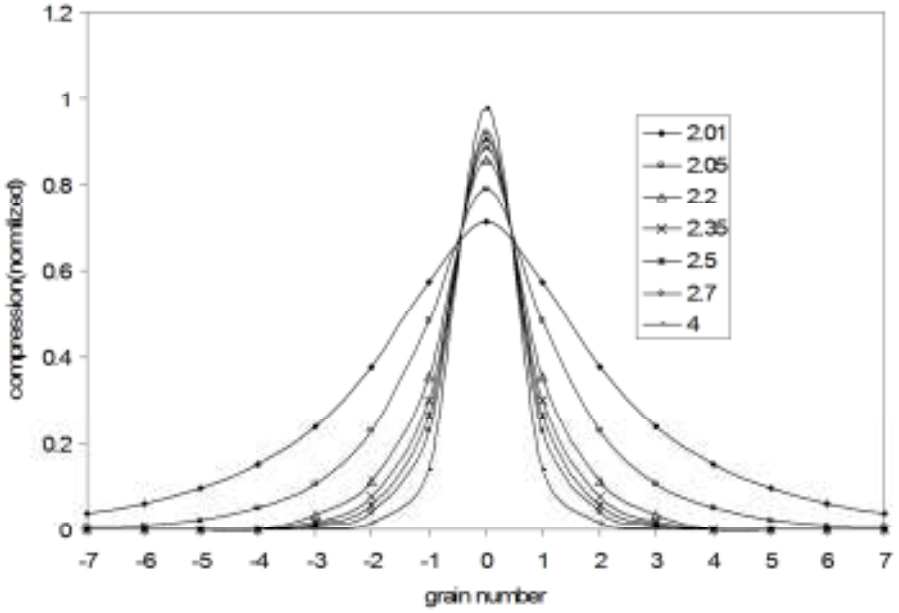

Fig.8. Analytical results of SWs (potential type) for set of different potential exponents.

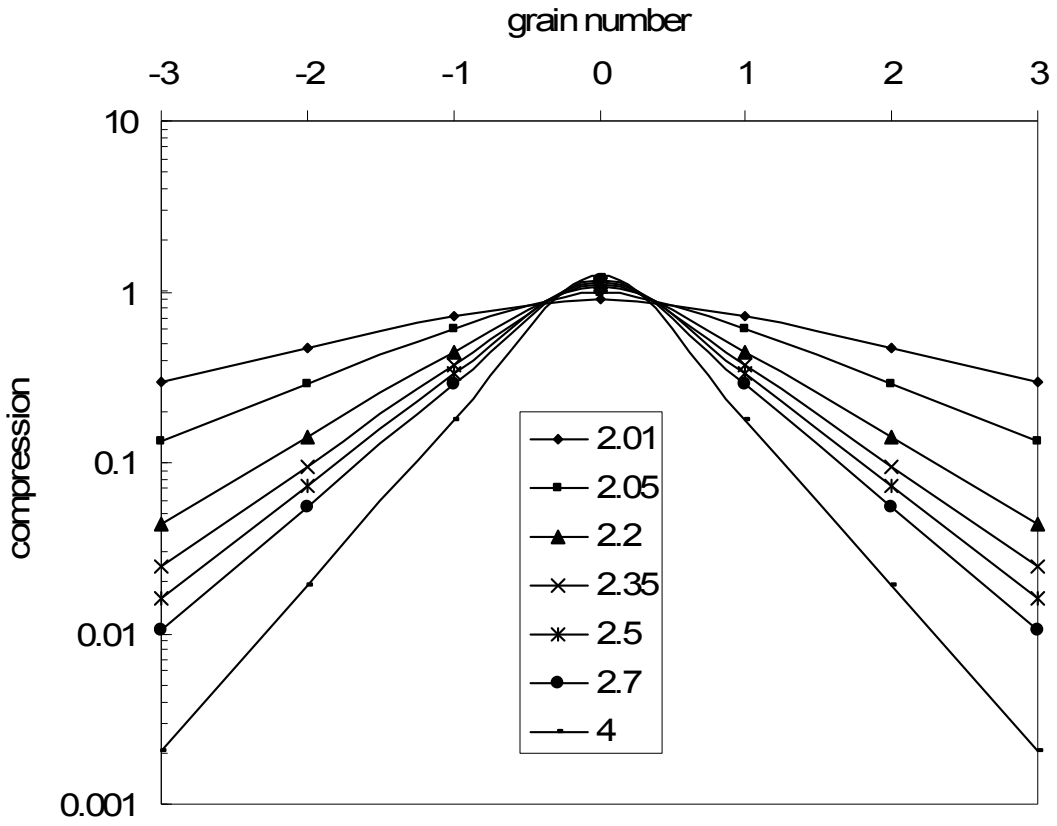

Fig.9. Log scale potential type SWs for set of different potential exponents.

Summary

To summarize this work, we conclude that the width of the SW in granular media exhibits an intrinsic power law dependence on the potential exponent *n*, i.e., $W \propto (n-2)^{-1/3}+1$. We have obtained agreement between the numerically and theoretically obtained values of this exponent. In monodispersed chains, *n* is the only parameter that controls the width of the SW. The physical meaning of the scaling law indicates that the width of the SW decreases much faster than the increase of the exponent *n* which is solely due to the nature of power law form of the potential. Therefore, when *n* increases, the energy transfer from one grain to the next becomes a progressively faster process. Such energy transfer tends to happen as a "one-shot deal". The exponent in scaling law (-1/3) must hence be greater then – 1 and less than zero.

References

Chatterjee, A., (1999), Phys. Rev. E59 5912.

Coste, C., Falon, E., Fauve, S., (1997), Phys. Rev. E 56 6104.

Goldstein, H., Poole, C. and Sofko, J., (2002), *Classical Mechanics*, Addison-wesley, San Francisco.

Hertz, H., J., (1881), Reine. Angew. Math. 92 156.

Landau, L.D., Lifshitz, E.M., (1970), *Theory of Continuum Media,* Pergamon, Oxford, p.30.

Lazaridi, A.N., Nesterenko, V.F., (1985), J. Appl. Mech. Tech. Phys. 26 405.

Nesterenko, V.F., (1994), J. Phys. IV 4 C8.729-6734.

Nesterenko, V. F., J. (1983), Appl. Mech. Tech. Phys. 5, 733.

Nesterenko, V.F., J. (1983), Appl. Mech. Tech. Phys. 24 733.

Nesterenko, V. F., J. (1994), Phys. IV C8 4,729

Pollard, H. (1964). *A sharp form of the virial theorem*. Bull. Amer. Math. Soc. **LXX**: 703-705

Russell, J.S., (1845), On Waves, Rept. Of the 14th Meeting of the British Association for the Advancement of Science, York, p.311.

Sinkovits, R.S., Sen, S., (1995), Phys. Rev. Lett. 74 2686.

Sen, S., Manciu M., A.J. ,(1999), Hurd, Physica A 274, 588.

Sen S., Manciu M., (2001), Phys. Rev. E 64 056605

Sen, S., et al., (2008), Solitary waves in the granular chain, Physics Reports.

Sen, S., Sinkovits, R.S., (1996), Phys. Rev. E 54 6857.

Sen, S., (2001), Phys. Rev. E 64, 056605.

Sokolow, A., Bittle E.G., Sen S., (2007), Europhys. Lett. 77 24002.

Spence, D.A., (1968), Proc. Roy. Soc. Lond. Ser. A 305 55.

Task (iii): In recent work using compressed granular alignments using reflective walls we have shown that there exists a critical loading where solitary waves and acoustic waves can coexist with the kinetic energy of the solitary wave being slightly larger than the average kinetic energy of the acoustic waves. Here we will attempt to develop a system where the solitary wave can be submerged under the noise by suitably modifying the system Hamiltonian in such a way that the added noise will not modify the coexisting phase (***Submerged Solitary Wave Problem***).

We came to understand that the real challenge was to make a stable solitary wave within the quasi-equilibrium phase and this is what is accomplished below. This work extends earlier work which hinted at a stable solitary wave in the quasi-equilibrium phase at critical loading where the harmonic and nonlinear forces are equally strong competitors. The work suggests that at such critical strengths, combination of nonlinear and linear forces can lead to unexpected nonlinear structures. The solitary wave can be submerged within noise without decay but this is not possible to do by using a single Hamiltonian. We present below in details our work on these stable solitary waves in the highly noisy quasi-equilibrium phase.

Long lived solitary wave in a 1D granular chain (Yoichi Takato, Edgar Avalos, Surajit Sen, SUNY Buffalo)

Abstract - Kinetic energy uctuations of a non-dissipative 1D granular chain held between perfectly reecting walls with various precompressions are numerically investigated. The dynamics of the system is explored for three cases, (i) for a *weakly* precompressed chain which admits only solitary waves that break down into secondary waves under wall collisions, which is consistent with other _ndings in the literature, (ii) for a *strongly* precompressed chain which exhibits mostly acoustic waves, and (iii) for a chain with *intermediate* precompression. Case (iii) accommodates a *nearly stable* solitary wave that travels unaffected through the acoustic waves and bounces back and forth between the walls for extremely long times.

Nesterenko was the first to report the existence of a traveling solitary wave (SW), i.e., a non-dispersive bundle of energy, in a 1D granular chain [1]. Since then, many theoretical and experimental studies on SWs have been carried out [2-4]. These studies have shed light on the intriguing characteristics of SWs in granular chains where grains repel via the strongly nonlinear Hertz potential [5]. One of the properties of SWs that was shown by computational simulations is as follows: a SW created out of _ function

perturbation to an edge grain of a chain breaks down into small secondary SWs due to interactions with walls or other SWs [6]. Although the secondary SWs carry much lower energy compared to the initial SW, they were experimentally found by Job *et al.* [4]. This breakdown of SWs eventually leads the chain to an interesting state as we shall see below.

Suppose that only one SW is created by a single initial impulse in the system. Now imagine that through wall collisions and collisions with one another many secondary SWs are born out of the single original SW. One would expect that eventually the chain will reach a state that will be full of secondary or low energy SWs. In this state, the secondary SWs will continue to exchange energy with one another via collisions. Energy conservation demands that eventually the secondary SWs will break down and reform at the same rate in the system. One may think that this is an equilibrium state by analogy with the equilibrium state of a spring-mass system whose potential is described by a harmonic potential. However, it turns out that the actual situation is quite different. For instance, the velocity distribution in this state is a Gaussian, whereas the equipartition theorem does not hold [7]. Further, in some cases the system's evolution appears to have no memory of the initial conditions whereas in others they do. In addition, when one investigates the fluctuations in kinetic energy for the Hertzian system in the equilibrium-like state one finds that the fluctuations are larger than those for a harmonic system [7]. The conclusion - this state is not the same as the equilibrium state in a harmonic chain. Therefore, this state was named as the *quasi-equilibrium* state to distinguish it from the ordinary equilibrium state [7, 8].

The dynamics of anharmonic systems has fundamental differences with respect to those of harmonic systems [9]. In particular, the Hertzian system has an important property which comes from the discreteness of the system; the weakly compressed system does not allow acoustic waves to propagate, these systems have been referred to as being in *sonic vacuum* [1]. On the contrary, the precompressed chain can admit acoustic waves [10] and strong precompression may suppress the nonlinearity and lead to a state with equipartitioned energy in the system like in a typical harmonic system. The role of intermediate precompression in the Hertzian system is not well understood.

In this paper we present our numerical study of kinetic energy fluctuations of a finite nondissipative linear chain made of Hertzian grains with precompression. The precompression ranges from weak enough so as to achieve sonic vacuum to strong enough so as to have acoustic waves in the system. We present evidence to show the existence of a striking long-lived SW at intermediate precompression.

Model and Method**:** We consider a 1D chain composed of N monodispersed spherical grains of radius R with rigid walls at both ends of the chain. These grains are barely in contact with one another at zero precompression. When two adjacent spherical grains are compressed, the repulsive potential is described by the Hertz potential [5],

$$V(\delta_{i,i+1}) = \begin{cases} a\delta_{i,i+1}^{n} & (\delta_{i,i+1} > 0 \\ 0 & (otherwise) \end{cases} \qquad (1)$$

where $n = 5/2$ and $\delta_{i,i+1} = 2R - (u_{i+1} - u_i)$ is the overlap between grain i and $i+1$ and u_i, u_{i+1} describe the positions of the centers of grain i and $i+1$, respectively. The prefactor a is given by $a = (2/5D)\sqrt{R/2}$, where D is determined by the grain's material properties; Poisson ratio σ and Young's modulus Y give $D = 3(1-\sigma^2)/2Y$. If the separation of two neighboring grains is greater than $2R$, they do not have physical contact and hence no force acts on the grains. For this study we set $a = 4.136 \times 10^7$N/m$^{3/2}$ and $R = 0.5$mm. This value of a corresponds to materials such as glasses.

The Hamiltonian is described by

$$H = \sum_{i=1}^{N} \frac{p_i^2}{2m} + \sum_{i=1}^{N} V(\delta_{i,i+1}), \qquad (2)$$

where p_i is the momentum of grain i, m is the mass of a grain and $V(\delta_{i,i+1})$ is the potential energy fue to the overlap. The equation of motion of grain i which is not next to a wall is given by

$$m\frac{d^2u_i}{dt^2} = na\{[\Delta + u_{i-1} - u_i]^{n-1} - [\Delta + u_i - u_{i+1}]^{n-1} \quad (3),$$

where the symbols are as defined above and Δ is the precompression.

A velocity perturbation is given to one end of the chain at $t = 0$ and it eventually develops into a traveling SW. The impact velocity is set to be $v_{imp} = 9.899 \times 10^{-2}$ m/s for all cases studied here. We solve the equation of motion using the velocity Verlet algorithm. The integration time step is $\Delta t = 10^{-9}$s.

Now, we define a time averaged fluctuation of the kinetic energy T of the chain as [7]

$$< F(t) > \equiv \sum_{\Delta t}^{N_{\Delta t}} \frac{|T_i(t) - <T>|}{N_{\Delta t}}, \qquad (4)$$

where $T_i(t)$is the instantaneous kinetic energy of the chain, $< T >$ is the average kinetic energy at $t \to \infty$, ,$N_{\Delta t}$ is the total number of time steps, and $F_i(t)$ is the instantaneous fluctuation of the kinetic energy.

Fluctuations of kinetic energy of a granular chain: We investigate how kinetic energy fluctuations behave as the precompression applied to the chain is varied for three different system sizes $N = 50$*;* 100, and 500.Fig. 1 shows the kinetic energy fluctuations obtained by our simulations. In each system size, the fluctuation is normalized by the value of the fluctuation at no precompression. In addition, the precompression Δ is nondimensionalized by grain radius $R = 0.5$ mm.

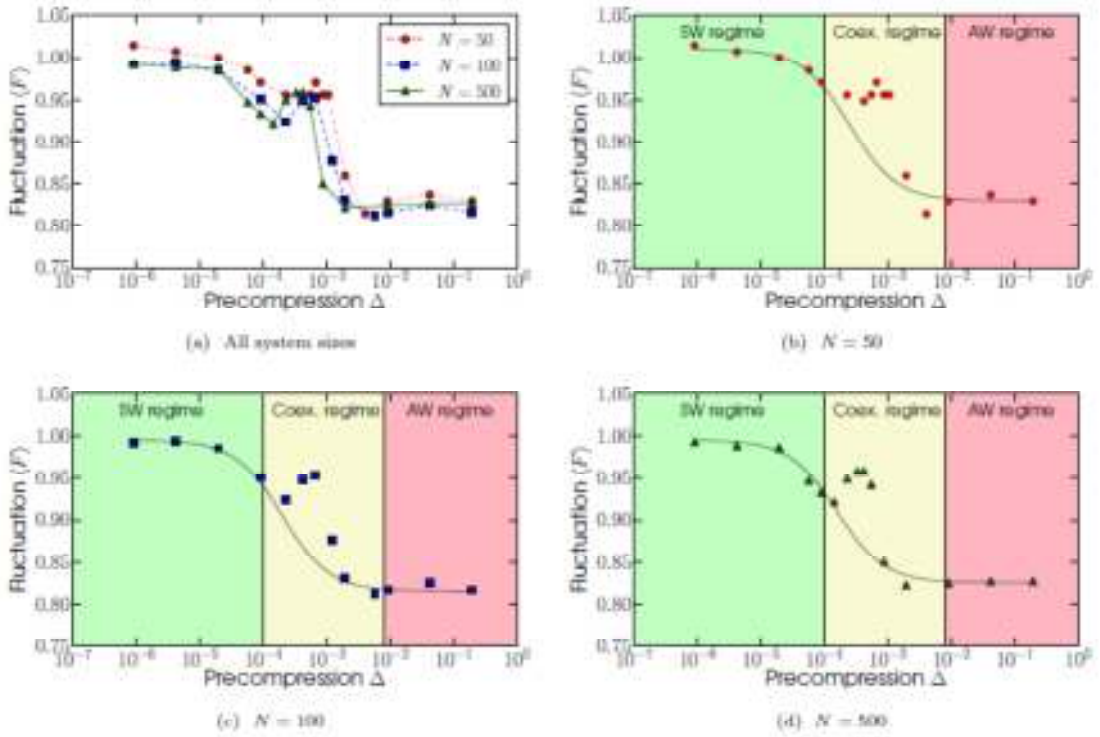

Fig. 1: Kinetic energy fluctuations of a granular chain obtained via simulations: The fluctuations are normalized by the fluctuation at precompression $\Delta = 0$ for each system size. (a) Fluctuations for $N = 50, 100, 500$; In (b), (c), and (d), each fluctuation in (a) is depicted separately by a fitting with Fermi-type function.

There are two distinct states at high and low precompressions in _g. 1. At the highest and lowest precompressions the fluctuations are almost at, however, the levels of the fluctuations are different in the two cases. The fluctuation for low precompression is 20% larger than that for high precompression and hence shows a clear difference between the two states. This is consistent with the results reported by Sen [7] that quasi-equilibrium state achieved in a weakly precompressed chain in small systems has more fluctuations by 12{27% compared to the equilibrium state. The equilibrium state corresponds to the state established in the strongly precompressed chain which allows mostly acoustic wave propagation.

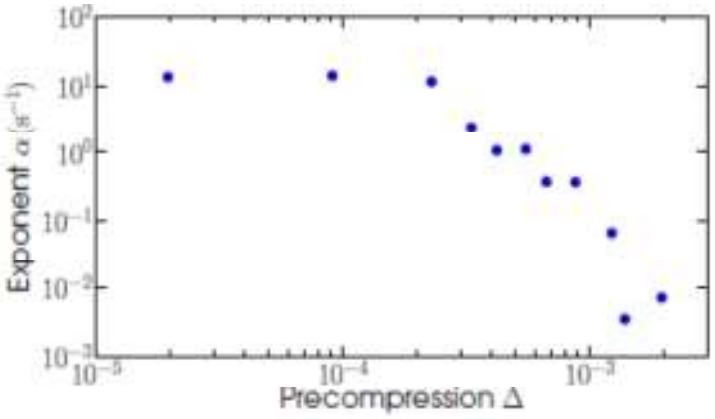

Fig. 2: The exponent α for the $N = 500$ system.

Another common feature to all the panels in fig. 1 is that the uctuations possess a broad peak at an intermediate precompression regime between 10^{-4} and 10^{-2}. Our simulation suggests that this broad peak in the fluctuations has to do with the fact that the fluctuations are yet to reach a steady state during the calculation of the fluctuations. Further, the inability to reach a steady state is because the kinetic energy at the precompression of interest changes extremely slowly in time. This is confirmed in Fig. 2, which shows an exponent α such that max $\{T_i(t)\} \propto t^{-\alpha}$. The maximum kinetic energy of the weakly compressed chain, which should be attributed to the initial solitary wave, decays very quickly, and its decay rate does not depend on the precompression, as shown in Fig. 2 as a large value that remains fixed for $\Delta < 2 \times 10^{-4}$. By contrast, the maximum kinetic energy of the chain with intermediate precompression decays slowly, and the rate becomes smaller with the increasing precompression around$2 \times 10^{-4} < \Delta < 1.5 \times 10^{-2}$. (see the negative slope in fig. 2). It indicates that uctuations of the kinetic energy at intermediate precompression could possibly be altered if the runs were even longer. Otherwise the fluctuation for each system size may converge to the smooth solid line shown in fig. 1, which is obtained using points not belonging to the peak. To run until convergence of the fluctuations, however, costs too much time as the exponent values show. For $\Delta = 9 \times 10^{-4}$, we ran the simulations about thirty times longer (a month in real time) than those for weakly compressed cases. Finally, for the strongly compressed chain, the exponent $\rightarrow \infty$ because an initial solitary wave which causes large uctuations may not exist. The system reaches a steady state at the very beginning of the runs, which will be presented below in fig. 3(e), and the average maximum kinetic energy remains unchanged in time.

So far, we have looked at the kinetic energy fluctuations of the system in the presence of precompression. The results, large fluctuations are seen for low precompression and small fluctuations are found for high precompression. These findings are not surprising because of the properties of the solitary waves in question. These waves break down into smaller waves and eventually form a steady state, which

leads to the quasi-equilibrium state for low precompression and at large precompressions the acoustic waves dominate, and these lead to the system being in a state with equipartitioned energy. What is unexpected is the odd slowing down of the system towards a steady state. This form of behavior is reminiscent of critical slowing down in systems undergoing phase transition [11] and we focus on this intriguing behavior below.

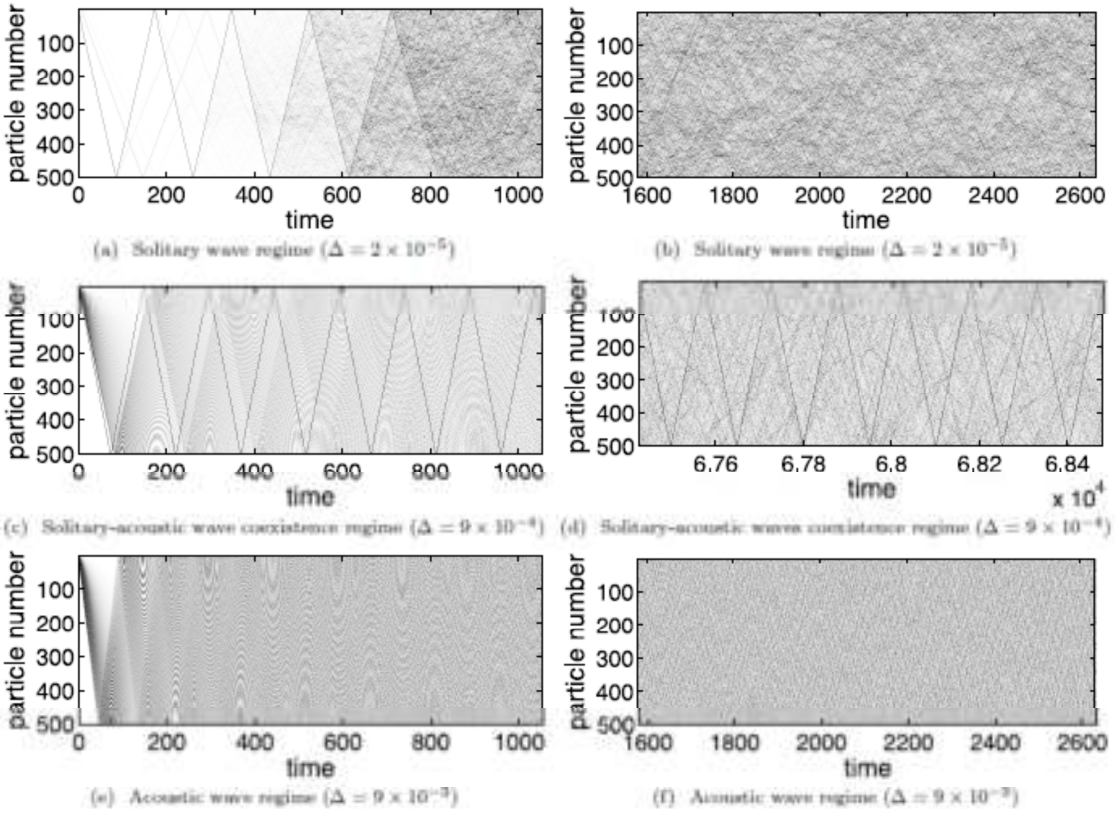

Fig. 3: Zigzag plot: These plots show distribution of the kinetic energy in space and time. The darker spot indicates higher kinetic energy. (a) and (b) $\Delta = 2 \times 10^{-5}$: A clear solitary wave is seen as straight lines, and then it disappears in the sea of secondary solitary waves.; (c) and (d) $\Delta = 9 \times 10^{-4}$: These have both features of (a) and (e) by looking at $t = 0$-100; (e) and (f) $\Delta = 9 \times 10^{-3}$: Acoustic waves quickly spread out over the whole chain.

A space-time plot of kinetic energy shown in gray scale (a “zigzag" plot) helps us easily visualize traveling SWs or acoustic waves in the chain in order to explore where the decay rate difference comes from. The darker spots in the plot represent higher kinetic energy. Such a spot may display a bundle of kinetic energy moving through the chain or how kinetic energy spreads in the chain. A SW, a bundle of kinetic energy, is shown as a sharp line in the zigzag plot. If a SW propagates from one end of the chain to the other end, the plot shows a straight line with a certain slope, which is the velocity of the SW. If kinetic energy is equally distributed, i.e., an equilibrium state is established, the plot shows a uniform gray pattern. The time shown in fig. 3 is normalized by the period of a harmonic oscillator $t_{harm} = 2\pi\sqrt{m/k}$, where k is the spring constant obtained by letting $k = \left(\frac{5}{2}\right) a$ with $\delta_{i,i+1} = R$.

Upon investigating the zigzag plots for the entire precompression window for an $N = 500$ system, we find that the patterns in the plots can be classified into three distinct types as shown in fig. 3. Fig. 3(a) and (b) represent precompression of$\Delta \leq 2 \times 10^{-5}$ (corresponding to weak precompression), fig. 3(c) and (d) represent $2 \times 10^{-4} \leq \Delta \leq 10^{-2}$ (corresponding to intermediate precompression), and fig. 3(e) and (f) represent $\Delta \geq 10^{-2}$ (corresponding to strong precompression). A zigzag plot for the weakly compressed chain in fig. 3(a) shows that a clear initial SW depicted by a thin solid line at the beginning ($t < 300$) travels in the chain; it starts to decay shortly after $t = 300$; it decays quickly, breaking down to secondary SWs around $t = 500$. In the case of the strongly compressed chain, the zigzag plot is drawn in fig. 3(e). It exhibits the behavior that is characteristic of that of sound waves. The initial perturbation spreads into the chain, and more than half of the grains in the chain have some kinetic energy by the time the wave front reaches the opposite wall. Therefore, it cannot be a SW. Moreover, at a later time the plot pattern turns

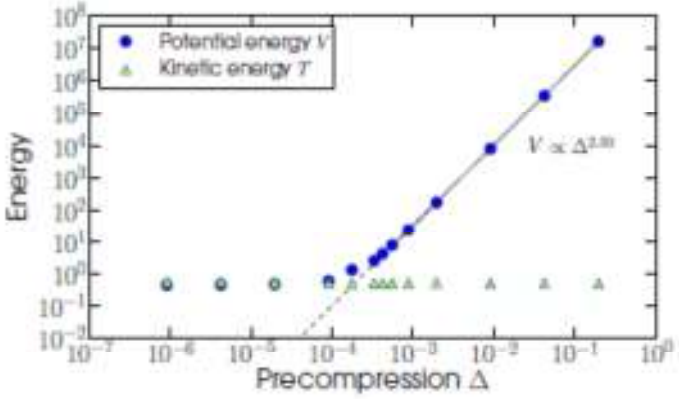

(a) Time averaged kinetic energy and potential energy

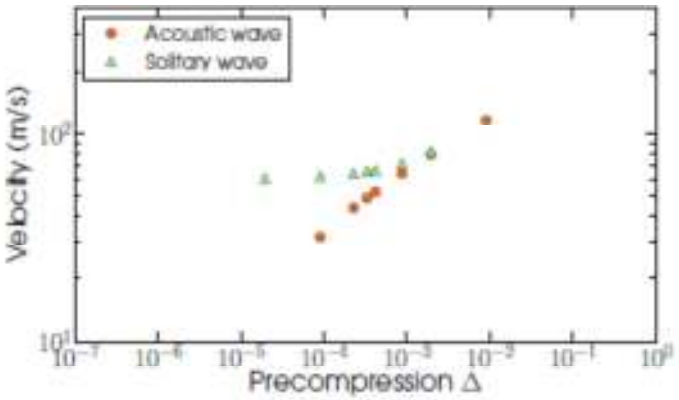

(b) Velocity of the solitary wave and the acoustic wave

uniformly gray, meaning that the system is now in a state with equipartitioned energy with seemingly no dependence on initial conditions and shows a Gaussian distribution of velocities centered around zero. Lastly, for the chain with intermediate precompression, a single SW and harmonic waves coexist as can

be seen in _g. 3(c). A SW represented by a sharp line in the plot is observed in fig. 3(a), and the gray pattern similar to the one shown in fig. 3(e) is also observed. Surprisingly, the SW lives for an extremely long time, until at least $t = 6.9 \times 10^4$, which is the end of the run. The SW does not attenuate much even though it repeatedly collides with the walls. The precompression exerted on the system seems to play an important role in suppressing the mechanisms that are associated with the decay of the SW via secondarySW formation and this seems to lead to the longevity of the SW.

Static and dynamic potential energy, and crossover precompression Δ_C: The precompression of the system is the only parameter varied for each system size in our study of fluctuations of kinetic energy. Impact velocity, grain size, grain mass, and all the material properties associated with this investigation are kept the same. The precompression is imparted to the system as static potential energy. Hence, the effect of precompression is similar to that of an external field that affects the system's dynamics. As we have seen above, the SW-acoustic wave coexistence state emerges at a certain precompression value and this may be a special state of the system. As argued extensively elsewhere [8], at zero precompression approximately 5/9 of the system's energy turns out to be kinetic and the remaining 4/9 to be potential. Such a system when subjected to a single velocity perturbation forms a solitary wave pulse that carries all of the system's energy. Precompression changes this behavior. Upon precompression, the system can possess more potential energy and when the amount of potential energy due to loading equals that due to the Hertzian interaction, a new state forms. In this state, the SW is present but the extra potential energy is used to generate acoustic waves which coexist alongside the SW. In _g. 4(a) the potential energy and the kinetic energy of the chain are shown as a function of the precompression. The potential energy at high precompression, $\Delta > 10^{-3}$, $\Delta > 10^{-3}$, is dominated by the precompression and that at low precompression, $\Delta < 10^{-4}$, is dominated by the Hertzian interacton. The coexistence regime begins where the the potential energy due to precompression becomes comparable with that due to Hertzian interaction. We assume that a way to estimate the strength of loading where the SW and the acoustic waves coexist is by defining a $\Delta_C$in such a way that potential energy from precompression equals the potential energy from Hertzian interactions. The details of this derivation are shown in Appendix A. The result of the crossover point is given by

$$\Delta_C = \left(\frac{2}{anN} < T >_t\right)^{1/n}, \qquad (5)$$

where $< T >_t$ is the time averaged kinetic energy of the chain. We perform a numerical calculation of the crossover point using the equation and the values obtained in our simulation for $N = 500$, $< T >_t = 5.2 \times 10^{-1}$ from our simulations, then we get $\Delta_C = 1.8 \times 10^{-4}$. It agrees with our simulation result of 1.9×10^{-4}. Furthermore, the peak shifts shown in fig. 1 can be explained by eq. (5) because the system size N is increased, then the crossover point becomes small, which also explains our simulation results.

The acoustic wave velocity goes up with increasing precompression in the coexistence regime as shown in fig. 4(b) and it approaches the solitary wave velocity almost independent of precompression. The solitary lives longer and longer as the two velocities come close together. Our investigations suggest that the wavelength of the acoustic waves is slightly larger than or of the same length as the typical width of the SW. We conjecture that the SWs are hence “invisible" to the acoustic waves and this may be why the acoustic waves cannot break down the SWs. However, when the precompression is further increased, the situation changes. The wavelength of the acoustic waves become smaller and these waves can now \pry open" the SWs which are quite a bit larger than them, thereby making them unstable. This is when the system shows acoustic like behavior.

Discussion

In this study, we have explored the problem of impulse propagation in precompressed grains that are held between rigid walls in a granular chain. At vanishingly small and zero loading we find that the SW breaks down into the quasi-equilibrium state that is characteristic of strongly nonlinear systems as discussed extensively in the literature now. It may be noted that in quasi-equilibrium, the energy is not equipartitioned in the system. The velocity distribution is Gaussian and in the case of the single impulse problem there appears to be no dependence on initial conditions [7]. When the precompression is sufficiently large such that the grains can only oscillate harmonically about their squeezed positions, the system behaves like a harmonic chain with N modes where N is the number of particles. Such a system of course satisfies the equipartition theorem, shows a Gaussian distribution of velocities and also has no dependence on initial conditions and can be regarded as in an equilibrium state. In the $N \to \infty$ limit though the distinction between the quasi-equilibrium and equilibrium phases becomes vanishingly small.

The striking result of this study is how the SW and acoustic waves *coexist* in this system for values of precompression between the two extremes. To our knowledge such a coexistence phase has not been seen in granular chains in earlier work. Here we find that there is a certain value of precompression, that depends on the Hertz potential and the system size, around which both the SW and acoustic waves coexist. This crossover point appears to be when the average grain-grain separation distance and the precompression become equal. Naturally in such a limit, the equation of motion becomes identical to that of the equation of motion at zero precompression upto a coupling constant. The wavelength of the acoustic waves seems comparable to the width of the SW. However, it remains to be understood why these SWs do not break down significantly via secondary SW formation.

The research has been supported by the Army Research Office.

REFERENCES

[1] Nesterenko V. F., J. Appl. Mech. Tech. Phys., 24 (1983) 773.

[2] Sinkovits R. S. and Sen S., Phys. Rev. Lett., 74 (1995) 2686; Sen S. and Sinkovits R. S., Phys. Rev. E, 54 (1996) 6857; Sen S., Manciu M., and Wright J. D., Phys. Rev. E, 57 (1998) 2386; Hinch E. J. and Saint-Jean S., Proc.R. Soc. Lond. A, 455 (1999) 3201; MacKay R. S., Phys. Lett. A, 251 (1999) 191; Chatterjee A., Phys. Rev. E, 59 (1999) 5912; Hasco et E., Herrmann H. J. and Loreto V., ibid., 59 (1999) 3202; Sen S., Manciu M., Sinkovits R. S. and Hurd A. J., Gran. Matt., 3 (2001) 33; Rosas A. and Lindenberg K., Phys. Rev. E, 69 (2004) 037601; Rosas A., Romero A. H., Nesterenko V. F. and Lindenberg K., Phys. Rev. E, 78 (2008) 051303.

[3] Coste C., Falcon E. and Fauve S., Phys. Rev. E, 56 (1997) 6104.

[4] Job S., Melo F., Sokolow A. and Sen S., Phys. Rev.Lett., 94 (2005) 178002; Job S., Melo F., Sokolow A. and Sen S, Gran. Matt., 10 (2007) 13; Daraio C., Nesterenko V. F., Herbold E. B. and Jin S., Phys. Rev. E, 73 (2006) 026610; Job S., Santibanez F., Tapia F. and Melo F., Ultrasonics, 48 (2008) 506.

[5] Hertz H., J. Reine Angew. Math., 92 (1881) 156; Goldsmith W., Impact (Edward Arnold, London) 1960.

[6] Manciu M., Sen S. and Hurd A. J., Phys. Rev. E, 63 (2000) 016614; Manciu F. S. and Sen S., ibid., 66 (2002) 016616.

[7] Sen S., Krishna Mohan T. R., and Pfannes Jan M.M., Phys. A, 342 (2004) 336; Krishna Mohan T. R. and Sen S. , Pramana J. Phys., 64 (2005) 423; Avalos E., Doney R. L. and Sen S., Chin. J. Phys., 45 (2007) 666; Wen Z.-Y., Wang S.-J., Zhang X.-M. and Li L., Chin.Phys. Lett., 24 (2007) 2887; ‼ Avalos E. and Sen S., Phys. Rev. E, 79 (2009) 046607; ‼ Avalos E., Sun D., Doney R. L. and Sen S., ibid., 84 (2011) 046610; Santibanez F., Munoz R., Caussarieu A., Job S. and Melo F., ibid.,84 (2011) 026604.

[8] Sen S., Hong J., Bang J., Avalos E., and Doney R., Phys. Rep., 462 (2008) 21.

[9] Toda M., Theory of Nonlinear Lattices, 2nd ed. (Springer, Berlin) 1981; Remoissenet M., Waves Called Solitons (Springer, Berlin) 1996.

[10] Nesterenko V. F., Dynamics of Heterogeneous Materials (Springer, New York) 2001.

[11] Halperin B. I. and Hohenberg P. C., Phys. Rev., 177(1969) 952

Task (iv): Here we will focus on studies where we shall explore heterogeneous granular alignments with the capability of creating significant hot spots or energy collection regions (***Granular Hot Spot Creation Problem***).

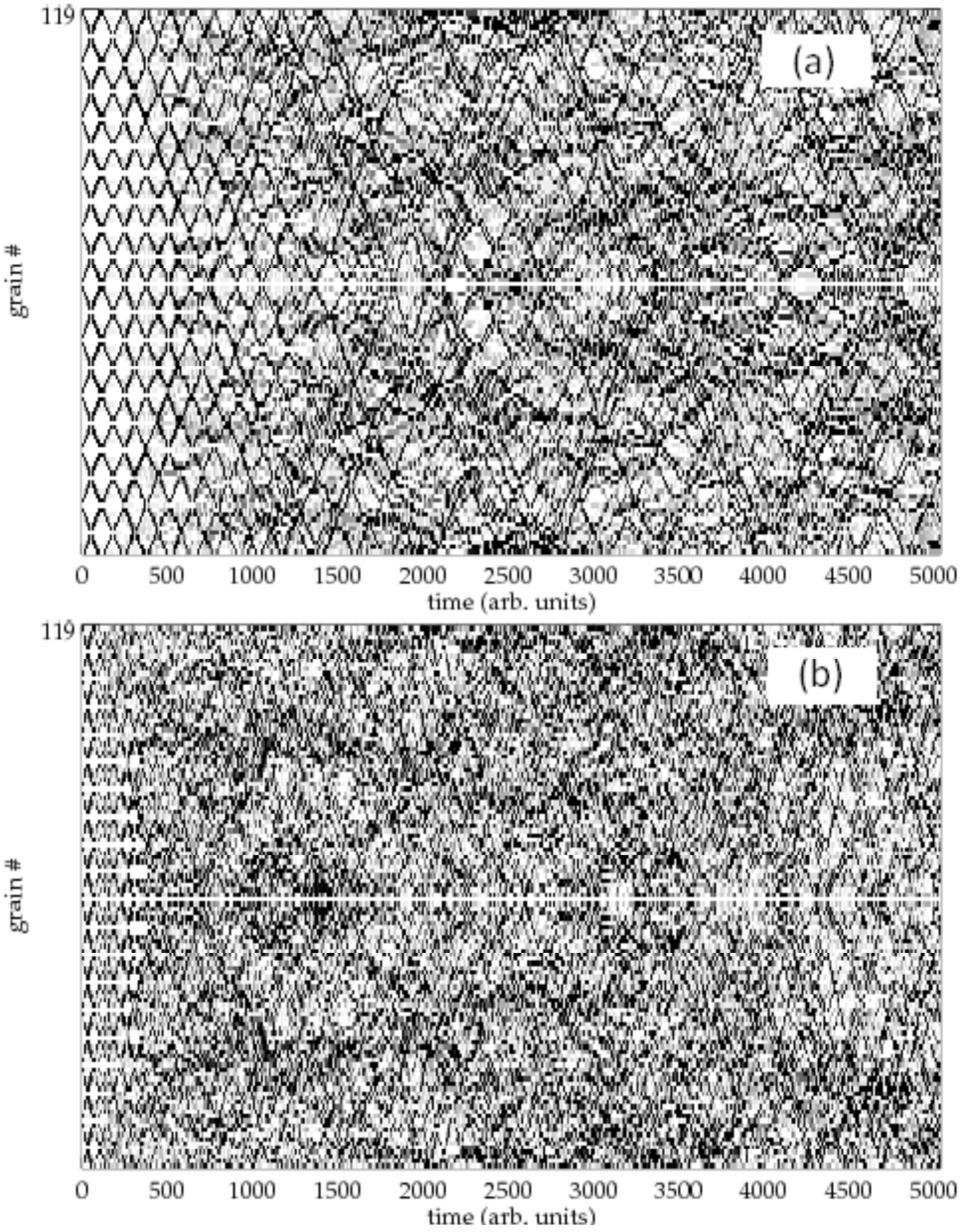

Figure 1: Here we show the time evolution of a 119 grain chain for n=2.5 in (a) and for n=2.1 in (b). Multiple perturbations are initiated at t=0. The dark patterns that emerge temporarily are the hot spots we were seeking. Further work to classify the intensity of the hotspots is now under way for driven, dissipative systems.

The granular hot spot creation problem is very much in progress and is likely to be for quite some years. This is a challenging problem that is similar to that of the emergence of rogue waves in oceans which form unexpectedly and are known to be a threat to vessels.

The PI and his team acknowledges STIR support for the work done so far which includes extensive simulations on the evolution of multiple perturbations initiated at the initial instant in a granular chain held between rigid walls. Studies have been done for systems with no dissipation. We found that when the initial perturbations are initiated in multiple grains, there is a strong chance that regions with very high kinetic energy will emerge unpredictably at late times. These high energy regions in space are temporary (see Fig. 1 above). Thus far we have found no way to predict the emergence of such hotspots though we find that many perturbations and specific boundaries are needed for these to likely form. Substantial progress on this problem is described in the manuscript included with this report which appeared in Physical Review E late in 2011 (E Avalos et al, Phys. Rev. **84**, 046610 (2011)). The next stage work will likely involve an experiment-theory collaboration which is needed for a breakthrough in our understanding – this phase is now under development.

Task (v): We will build on previous studies on mechanical energy propagation in confined 3D granular beds of mono-sized Hertz spheres to extend our code to incorporate the presence of air in interstitial space (***3D Granular Bed with Air Problem***).

In the STIR proposal, the PI had claimed that work will be started in coding the case of 3D granular systems with interstitial fluids in them. This work breaks into new territory in modeling granular beds with a molecular fluid in the interstitial spaces where the calculations are done at a length scale of 10s of microns to a few millimeters. Matt Westley (PhD student) and the PI initially started this work in close dialog with the Livermore geophysics group's Dr Otis Walton and Dr Eric Herbold. It turned out, however, that essentially no progress had been made on this problem that is very useful beyond the work of Professor A.J.C. Ladd of the University of Florida, which used hydrodynamic assumptions that mimic a dilute, incompressible gas.

Our work has hence focused on the dynamics of a gas in the interstitial space between grains. The focus has been on developing a Molecular Dynamics based calculation scheme that describes a Lennard-Jones fluid. The molecules suffer elastic collisions with the walls, which are made of surfaces of the grains that define the interstitial space as detailed below.

1. Introduction

The properties of energy transmission through granular media are generally not well understood. We intend to build a computational model for the propagation of mechanical energy through such materials as dirt, mud, and sand. This is to be accomplished by first exploring the simplest case of two grains impacting while cushioned by an interstitial fluid (whether air, water, or something else) in full detail. By constructing a molecular dynamics simulation from the ground up, we should be able to extract enough relevant information to make useful approximations for many grains. These approximations, should they be computationally inexpensive enough, will allow us to create a full model for energy propagation through large beds of grains with interstitial fluids such as air, water etc.

2 Current progress

Thus far we have considered the first part of this study. The molecular dynamics program we use is the Large-scale Atomic/Molecular Massively Parallel Simulator (LAMMPS), developed by

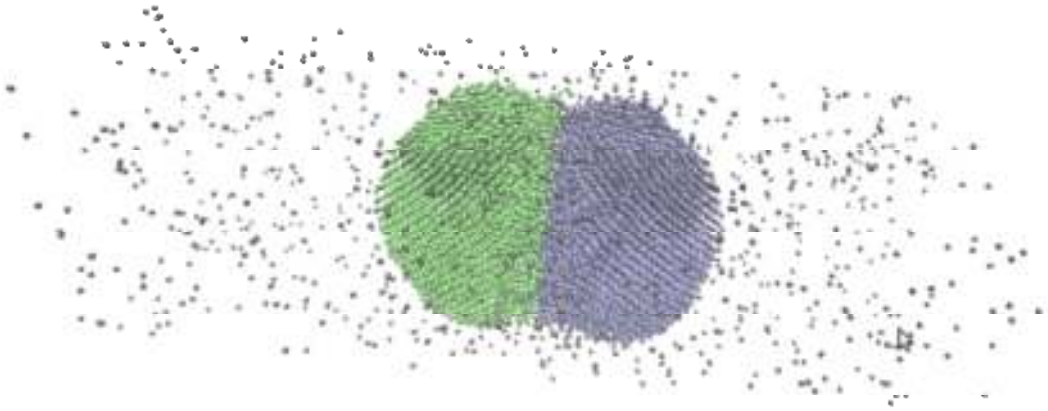

Figure 1: A side view of the collision of two clusters. The walls of the containing cylinder have been made invisible.

Sandia National Laboratories [1]. With LAMMPS, we have constructed the grain collision as follows: Take a large collection of Lennard-Jones (LJ) particles in equilibrium at a known temperature, and cut two spheres from this material. These are to be our grains. Then, place these grains in a tube or cylinder which is a tight fit around them. (We do this to follow more closely the experimental study by Job *et. al.* [2].) Then, we place an interstitial fluid consisting of single high-temperature light LJ particles inside of this cylinder. The grains are then each given an initial velocity towards the center of the cylinder where they collide in a head-on collision.

We record all relevant data from this collision, in particular the force between the two grains (as measured by summing the forces between each particle within the clusters) and the overlap between the grains for many different runs. Currently a single run involves the collision of two 1500-particle grains at a given initial velocity, and takes approximately two minutes of computer time to run with acceptable numerical error bounds. The next step is to take all of the data that has been generated in this way and analyze it to extract the force law between the two spheres. Ordinarily, we would expect a Hertz law for the sphere contact, but the interstitial fluid has proven to have a large effect on the force law [2]. We hope to recover the linear approximation made by Job *et. al.* [2] for this collision.

[1] S. Plimpton, J. Comput. Phys, **117**, 1 (1995).

[2] S. Job, F. Santibanez, F. Tapia, F. Melo, Ultrasonics **48**, 506 (2008).